



**TECHNICAL COMPARISON BETWEEN TWO STEAM GENERATION  
CONNECTIONS USING HIGH TEMPERATURE HEAT PUMPS**

Lappeenranta–Lahti University of Technology LUT

Bachelor's Programme in Energy Technology, Bachelor's thesis

2026

Eeli Leskinen

Examiners: Associate Professor Antti Uusitalo

Associate Professor Liyao Xie

## ABSTRACT

Lappeenranta–Lahti University of Technology LUT

LUT School of Energy Systems

Energy Technology

In co-operation with partner university: Hebei University of Technology

Eeli Leskinen

## **TECHNICAL COMPARISON BETWEEN TWO STEAM GENERATION CONNECTIONS USING HIGH TEMPERATURE HEAT PUMPS**

Bachelor's thesis

2026

62 pages, 20 figures and 14 tables

Examiners: Associate Professors Antti Uusitalo and Liyao Xie

Keywords: steam generating heat pump, mechanical vapor recompression, flash tank, steam generator, waste heat utilization, heat pump market potential, electricity-to-gas price ratio, refrigerant, PFAS

The purpose of this thesis was to compare two steam generation connections in terms of steam generation capacity per unit and overall system performance (COP). In the first connection, a closed-cycle compression heat pump was connected to a separate flash vessel, where steam was generated at 85 °C and then further compressed to three different pressure levels: 1,43, 3,62 and 6,18 bar(a), utilizing mechanical vapour recompression (MVR) technology. In the second connection, steam was generated directly in a plate & shell heat exchanger operating as the condenser of the heat pump at 110 °C. Similarly, the steam was further compressed by radial MVR compressors to 3,62 and 6,18 bar(a). Three different closed-cycle compression heat pump configurations were used, and three refrigerants were selected for the comparison: R1234ze(E), R1233zd(E), and R600a (isobutane). The results demonstrate that generating steam in a flash tank operating under vacuum conditions can have a significant advantage over the direct steam generation connection, achieving a 0,20 to 0,75 unit higher COP, depending on the evaporation temperature, refrigerant, and heat pump configuration. The comparison was carried out as a theoretical calculation. However, the heat pump compressor performance values were obtained from two compressor manufacturers' software tools, and the MVR performance values were provided by a technology supplier. In addition to the technical comparison, this thesis also presents information on high-temperature heat pumps, potential refrigerants, and the market potential of the technology in question.

## SYMBOLS AND ABBREVIATIONS

### Roman characters

$c$	specific heat capacity	kJ/kg
$h$	enthalpy	kJ/kg
$\dot{m}$	mass flow rate	kg/s, kg/h
$n$	number of heat pumps	pcs
$P$	power	kW
$p$	pressure	bar
$Q$	heating / cooling power	kW, MW
$T$	temperature	°C, K
$v$	specific volume	m <sup>3</sup> /kg
$x$	water vapor fraction	%

### Greek characters

$\varepsilon$	pressure ratio	bar/bar
$\eta$	efficiency	%
$\tau$	multiplier (freq. conv.)	%

### Subscripts

1	Enthalpy before compressor [kJ/kg]
2	Enthalpy after compressor [kJ/kg]
2s	Enthalpy after isentropic compression [kJ/kg]
circ	Circulating water in flash connection
el	Electric power

inj            Injected water between MVR compressors

#### Abbreviations

CFC	Chlorofluorocarbon
COP	Coefficient of performance
ECHA	European Chemicals Agency
ECO	Economizer
GWP	Global warming potential
HC	Hydrocarbon
HCFC	Hydrochlorofluorocarbon
HCFO	Hydrochlorofluoroolefins
HFC	Hydrofluorocarbons
HFO	Hydrofluoroolefins
IHX	Internal heat exchanger
MVR	Mechanical vapour recompression
PFAS	Per- and polyfluoroalkyl substances
PFC	Perfluorocarbon
TFA	Trifluoroacetic acid
TRL	Technology readiness level
ODP	Ozone depletion potential

## Table of contents

Abstract

Symbols and abbreviations

Declarations

1	Introduction .....	7
2	Market potential of high-temperature and steam-generating heat pumps .....	9
2.1	Industrial applications .....	10
2.2	Industrial waste heat sources .....	12
2.3	Electricity-to-gas price ratio .....	15
3	Steam generating heat pump .....	18
3.1	Heat pump theory .....	18
3.2	Working principle of a steam generating heat pump .....	20
3.3	Refrigerants .....	23
3.3.1	The working fluid of a steam generating heat pump .....	24
3.3.2	Refrigerants selected for the technical comparison .....	27
3.3.3	The future of refrigerants .....	29
3.4	Mechanical vapor recompression .....	29
4	Technical comparison .....	34
4.1	Heat pump connections .....	34
4.1.1	Operating values of refrigerants .....	35
4.2	Calculations .....	38
4.2.1	Flash tank vs. Steam generator .....	41
4.2.2	MVR after steam generation .....	44
5	Results and analysis of technical comparison .....	46
5.1	Steam generating heat pumps .....	46
5.2	Total system performance (Steam generating heat pump + MVR) .....	50
6	Conclusions .....	55
	References .....	58

## DECLARATIONS

### **Turnitin**

The originality of this thesis has been reviewed with the Turnitin similarity checking service.

### **AI usage**

The author of the thesis, Eeli Leskinen, used the following AI-tools during the preparation of the thesis:

1. ChatGPT 5.1/5.2
  - a. Purpose of use: To ensure linguistic accuracy throughout the writing process.
  - b. Explanation of the use of the tool: ChatGPT 5.1/5.2 was used solely for linguistic purposes, including translation work, and ensuring grammatical accuracy and consistency. All the content, including analysis, interpretations, and conclusions were produced independently by the author.

### **Responsibility**

The author, Eeli Leskinen, takes full responsibility for the content of this thesis and has reviewed and edited the content generated by the possible use of AI tools.

# 1 Introduction

Producing steam without fossil fuels such as natural gas is a topic of continuous discussion. Steam generating heat pumps intended to produce low and medium temperature heat (up to +300 °C) have developed significantly in recent years. Steam generating heat pumps designed for temperatures below +200 °C have partly already advanced to production, although ready-made heat pump solutions remain scarce, as the technology often requires precise customization depending on the application. Extensive development work is being carried out so that steam heat pumps could be commercialized for low-temperature use and current steam boilers, which often rely on fossil fuels, could be replaced.

The key advantage of industrial heat pumps is their ability to utilize waste heat generated on-site and upgrade it to a higher temperature level for the process. In Europe and in Finland, large amounts of recoverable waste heat are generated annually, most of which remains unused. The temperatures of these waste heat sources are mainly below 80 °C and require careful assessment and system integration to be utilized efficiently in heating.

This bachelor's thesis compares two different configurations for producing process steam. In the first configuration, steam is produced under vacuum in a separate steam separator (flash tank), from which its pressure and temperature are raised to the desired level using Mechanical Vapour Recompression (MVR) compressors. In the second configuration, steam is produced directly in the condenser of the heat pump, which in this case functions as a steam generator. After the steam generator, the steam is directed to the MVR system for pressure boosting. In this thesis, steam production is examined up to a maximum absolute pressure of 6,18 bar (+160 °C). The steam production analysis for the heat pumps is carried out using the sizing programs of two different compressor manufacturers. For the MVR system, the performance values used in the analysis have been obtained from equipment manufacturers.

The thesis does not examine in detail the current state of research on steam generating heat pumps. Solla (2025) provides a comprehensive research review of various high-temperature heat pumps using multiple refrigerants. Rontti (2024) has also reviewed studies related to different process configurations from recent years. However, the thesis presents solutions

already in industrial use from the perspective of MVR and aims to provide a comprehensive overview of the potential of MVR technology alongside a heat pump. The sources used in the thesis are listed in the reference list, excluding information obtained from equipment suppliers. These are, however, mentioned in the text when referenced.

The thesis consists of a literature section reviewing the current market situation of industrial heat pumps, heat pump theory, the theory of refrigerants suitable for high-temperature heat pumps, and the basic principles of MVR systems. The section discussing market potential highlights industrial processes whose operating temperatures are favourable for steam generating heat pumps. In addition, it presents typical waste heat sources and temperatures and estimates the magnitude of investments related to heat pump integration based on, among other factors, the ratio between electricity and natural gas prices. After the literature section, a profitability analysis is carried out comparing the efficiency and economic feasibility of the steam production configurations when evaporation temperatures vary between 15 and 70 degrees Celsius.

This thesis is part of Calefa Oy's product development and serves as a tool for the company in the marketing of steam heat pumps. In addition, the aim of the thesis is to provide useful information in the light of recent studies on refrigerants suitable for high-temperature applications and their associated limitations. The thesis seeks to provide the company with an understanding of the conditions under which each steam configuration is profitable to use in terms of efficiency and steam production capacity.

## 2 Market potential of high-temperature and steam-generating heat pumps

Globally, investments aimed at promoting the green transition in energy production exceeded investments in systems using fossil fuels in 2016. At present (2025), the total value of investments in systems utilizing renewable energy sources is twice as high compared to those relying on fossil fuels such as coal, natural gas, or oil. (IEA 2025) The share of heat pumps has increased significantly alongside the growing popularity of other renewable energy sources over the last decade. (EHPA 2025c)

The share of combustion in energy and electricity production will decrease in the future. This is because alternative technologies enable heat and electricity production without combustion and at lower costs. Although CO<sub>2</sub>-neutral fuels such as biofuels and the continuously developing biogas and hydrogen plants will form a significant share of future energy production, alternative technologies are also being continuously developed. At the so-called low-temperature level (below +200 °C), heat pumps are considered as potential solutions for industrial needs. High-temperature heat pumps can upgrade waste heat into steam for various process requirements. (Rannikko 2023)

The main advantage of heat pumps compared to other methods is their ability to utilize waste heat without CO<sub>2</sub> emissions. Zero-emission operation is possible if the electricity used by the heat pump is produced from renewable energy sources such as solar or wind power. Another advantage of heat pumps is their ease of control and compact size. (Rannikko 2023) As a result of these advantages, a heat pump system is a flexible choice that can operate as the primary system, or as a so-called preheater supporting an existing heating system.

Looking to the future, high-temperature heat pumps are among the most promising technologies for replacing industrial boilers that use fossil fuels. Steam heat pumps enable the utilization of process waste heat, making processes more energy-efficient and improving the overall heat management of the system. Heat pumps that operate solely on electricity can significantly reduce greenhouse gas emissions and support the achievement of carbon-neutrality targets. (Zini et al. 2024) Small and medium-sized companies that purchase steam produced from fossil fuels may face considerable challenges if the price of natural gas

becomes too high. Heat pump technology helps companies achieve self-sufficient heat production and thereby increases security in ensuring stable production. (Arpagaus & Bertsch n.d.)

## 2.1 Industrial applications

In Europe, the industrial demand for thermal energy amounts to approximately 3000 TWh per year. Around two thirds of this are consumed for process heating, which is typically produced using fossil fuels. (HPTTCP 2023) As a result, the majority of industrial CO<sub>2</sub> emissions arise specifically from heating processes. High-temperature industrial heat pumps can be used to produce process heat and thereby make industrial heating processes rely more on low-emission technology and energy production. (HPTTCP 2023) Figure 1 presents the energy demand of European industry and the temperature ranges of process heating, as well as the current energy sources used for heat production.

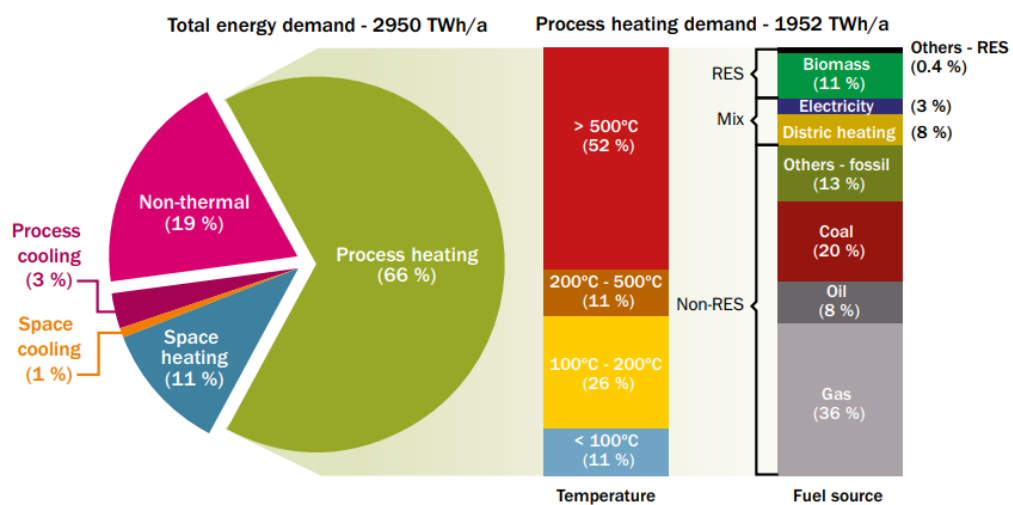


Figure 1. Energy demand in European industry and the share of process heating, temperature levels and heat sources (de Boer et al. 2020).

From the figure it can be seen that one quarter of Europe's process heating demand falls within the 100–200 °C temperature range. More than one third of process heating demand is below 200 °C. However, more than 70% (in 2020) of produced process heat was generated directly using fossil fuels. The figure demonstrates a very high potential for high-temperature heat pumps in process heat production. Nevertheless, in view of current high-temperature

heat pump technology, heat sinks above +150 °C pose challenges, and only a limited number of systems are currently in operation. (Arpagaus et al. 2018)

Possible applications identified for heat pumps in various industrial sectors include drying, cooking, bleaching, pasteurisation, sterilisation, casting, dyeing, and distillation processes. These processes are commonly used in the food and beverage industry, the metal industry, the plastics and wood industries, the textile industry, and the pulp and paper industry. (HPTTCP 2023) The heating demands of different industries and the required processes are presented in Table 1.

Table 1. The temperature demand of various industrial processes (Arpagaus et al. 2018).

Sector	Process	Temperature										[°C]	
		20	40	60	80	100	120	140	160	180	200		
Paper	Drying												90 to 240
	Boiling												110 to 180
	Bleaching												40 to 150
	De-inking												50 to 70
Food & beverages	Drying												40 to 250
	Evaporation												40 to 170
	Pasteurization												60 to 150
	Sterilization												100 to 140
	Boiling												70 to 120
	Distillation												40 to 100
	Blanching												60 to 90
	Scalding												50 to 90
	Concentration												60 to 80
	Tempering												40 to 80
	Smoking												20 to 80
Chemicals	Distillation												100 to 300
	Compression												110 to 170
	Thermoforming												130 to 160
	Concentration												120 to 140
	Boiling												80 to 110
Automotive	Bioreactions												20 to 60
	Resin molding												70 to 130
Metal	Drying												60 to 200
	Pickling												20 to 100
	Degreasing												20 to 100
	Electroplating												30 to 90
	Phosphating												30 to 90
	Chromating												20 to 80
Plastic	Purging												40 to 70
	Injection molding												90 to 300
	Pellets drying												40 to 150
Mechanical engineering	Preheating												50 to 70
	Surface treatment												20 to 120
Textiles	Cleaning												40 to 90
	Coloring												40 to 160
	Drying												60 to 130
	Washing												40 to 110
Wood	Bleaching												40 to 100
	Glueing												120 to 180
	Pressing												120 to 170
	Drying												40 to 150
	Steaming												70 to 100
	Cocking												80 to 90
	Staining												50 to 80
Several sectors	Pickling												40 to 70
	Hot water												20 to 110
	Preheating												20 to 100
	Washing/Cleaning												30 to 90
	Space heating												20 to 80

In table 1, the colours of the boxes indicate the technology readiness level (TRL) of heat pumps in that specific industrial process. The light grey boxes represent lower temperatures where heat pumps are already utilised in industrial applications. The black and dark grey

boxes represent prototypes used in high-temperature applications. The table shows that industry has a very wide range of needs for process heating precisely in the range where heat can be produced using heat pumps. According to Marina et al. (2021), the most suitable applications for high-temperature heat pumps can be found in the pulp and paper industry, the chemical industry, and the food industry.

## 2.2 Industrial waste heat sources

One of the key advantages of heat pumps is the utilization of waste heat in process heating. To meet the industrial demand for process heating through heat pump technology, a suitable heat source with an appropriate temperature level is also required. Figure 2 represents COP values of heat pumps used in industrial applications as a function of the temperature lift between the heat source and the heat sink ( $\Delta T_{lift}$ ). In this case, the heat sink temperature has been 140 °C. If the lift is 100 °C or more, according to figure 2, the COP the high-temperature heat pump can reach is only around 2, and the investment might no longer be economically viable. For this reason, a detailed assessment of both heat sinks and heat sources must be carried out for each industrial site.

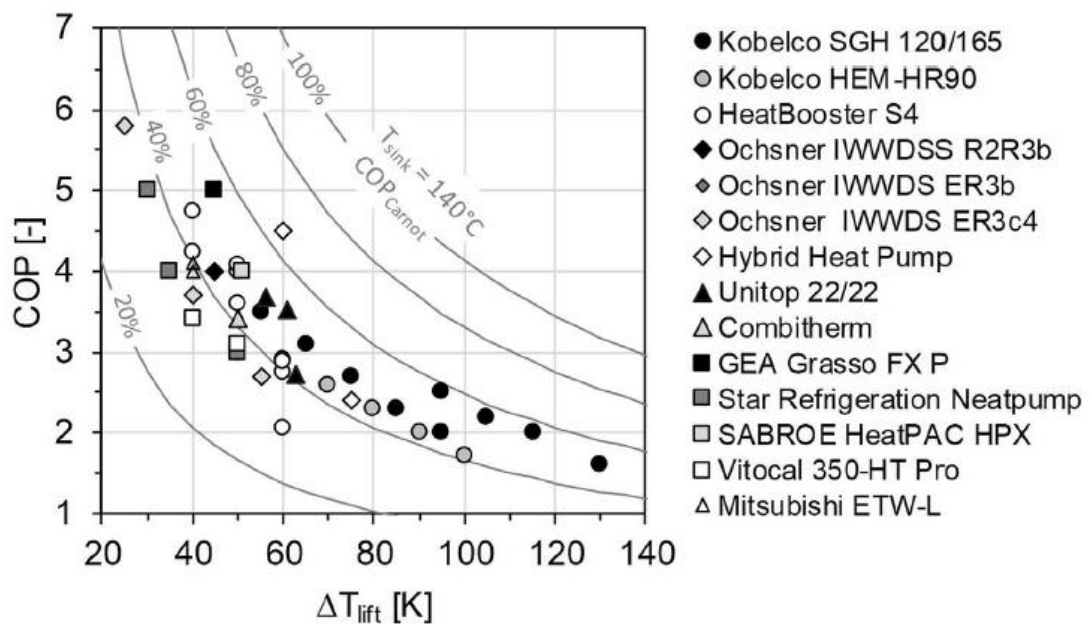


Figure 2. COP values of different industrial heat pumps as a function of temperature lift (Arpagaus et al. 2018).

The figure shows how the COP value decreases as the temperature lift increases. The grey curves in the figure illustrate the actual COP values compared to the theoretical COP calculated according to the temperatures of the heat source and heat sink. According to the figure, even under the best circumstances, modern heat pumps are currently able to achieve approximately 50–60% of the theoretical COP value.

Marina et al. (2021) studied the process waste heat produced by four industrial sectors (pulp and paper, chemical, food and beverage, and refineries). In Figure 3, the annual total amount of waste heat sources is presented as a function of temperature levels. The estimated amount of waste heat in these industrial sectors is 1130 PJ per year, of which waste heat below 150 degrees accounts for 92% (1039 PJ).

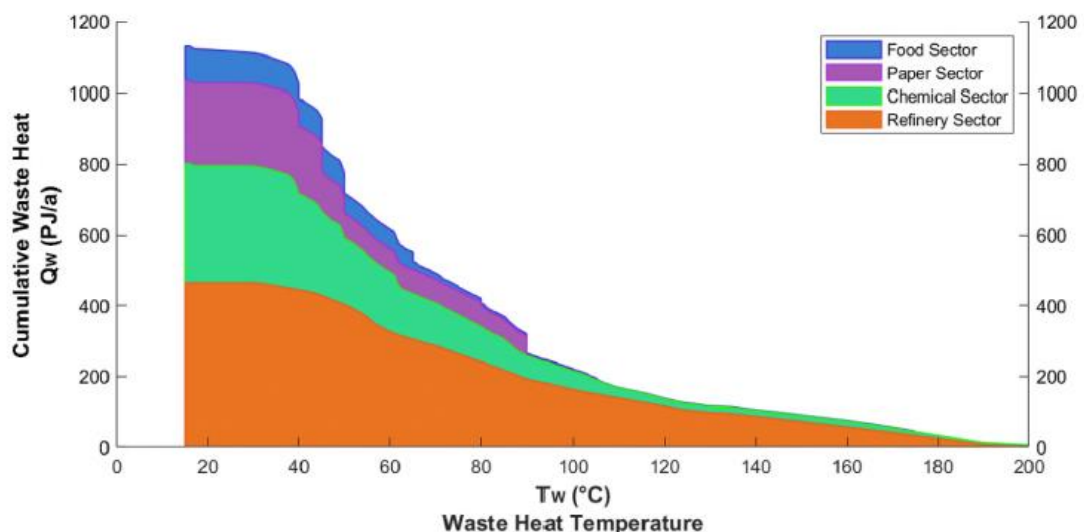


Figure 3. Annual cumulative waste heat amount as a function of waste heat temperature in four different industrial sectors (Marina et al. 2021).

From the figure it is clearly visible that the largest share of waste heat is at approximately 15–40 °C. This type of waste heat is found in all industrial sectors. Based on the study, the largest amount of waste heat is generated in the refinery industry, where waste heat sources of up to 180 °C can be found. Each industrial sector has waste heat up to around 100 °C. Typically, waste heat between 40 and 100 °C is in the form of moist air or condensate originating from process heating (Marina et al. 2021). When considering the maximum possible temperature lift of heat pumps, these waste heat sources are the most viable to utilise for the production of low-pressure steam. In the case of moist air, the water dew point must

be taken into account, at which the moist vapour condenses into liquid water. (Marina et al. 2021)

According to the Ministry of Economic Affairs and Employment (2025), Finnish industry generates approximately 15 TWh of recoverable waste heat annually. According to a study conducted by Motiva in 2019, the largest shares of waste heat originate from the food industry, metal processing, the forest industry, and the chemical industry. The forest industry in this context includes both the sawmill and wood product industry, as well as the paper and cardboard industry. Slightly more than half of the waste heat sources are below 55 °C, and slightly less than half above 55 °C. Table 2 below presents waste heat sources in different temperature ranges.

Table 2. Waste Heat Sources in Finnish Industry by Temperature Level (Adapted from Motiva 2019).

<i>Temperature level</i>	<i>Sources of waste heat</i>
<i>&lt; 50°C</i>	Cooling water from various processes Condensation energy from mechanical cooling Exhaust airflows related to processes
<i>50–100°C</i>	Cooling water from various processes Exhaust vapors Cooling of oil-lubricated air compressors
<i>&gt;100°C</i>	Flue gases Hot exhaust gases from processes

As a general rule, waste heat above 100 degrees occurs in industry only when the production process is connected to a power plant. However, various airflows, cooling and heating process condensates, and exhaust vapours provide a good market opportunity for industrial heat pumps in Finland.

The continuously increasing number of data centres also constitutes a significant source of waste heat both in Finland and globally. This waste heat typically exists at temperatures of

25–35 °C and 50–60 °C, depending on the data centre’s cooling system, and can be utilised for example in district heating production (Wang et al. 2024).

### 2.3 Electricity-to-gas price ratio

One of the factors that most strongly influences investment decisions regarding heat pump systems is the ratio between the price of electricity and the price of fossil fuels, typically natural gas. Arpagaus (2024) mentioned that the attractiveness of the heat pump market depends on the magnitude of this ratio. In general, heat pump systems are an appealing investment option when the price of electricity is relatively low compared to the alternative. (deBoer et al. 2020) However, it is worth noting that even if the ratio is higher in some countries, investment decisions are also affected by the need for electricity and gas, the buyer’s willingness to invest in green energy, and various other individual factors. Figure 4 presents the ratio between electricity prices and natural gas prices for industry in different European countries.

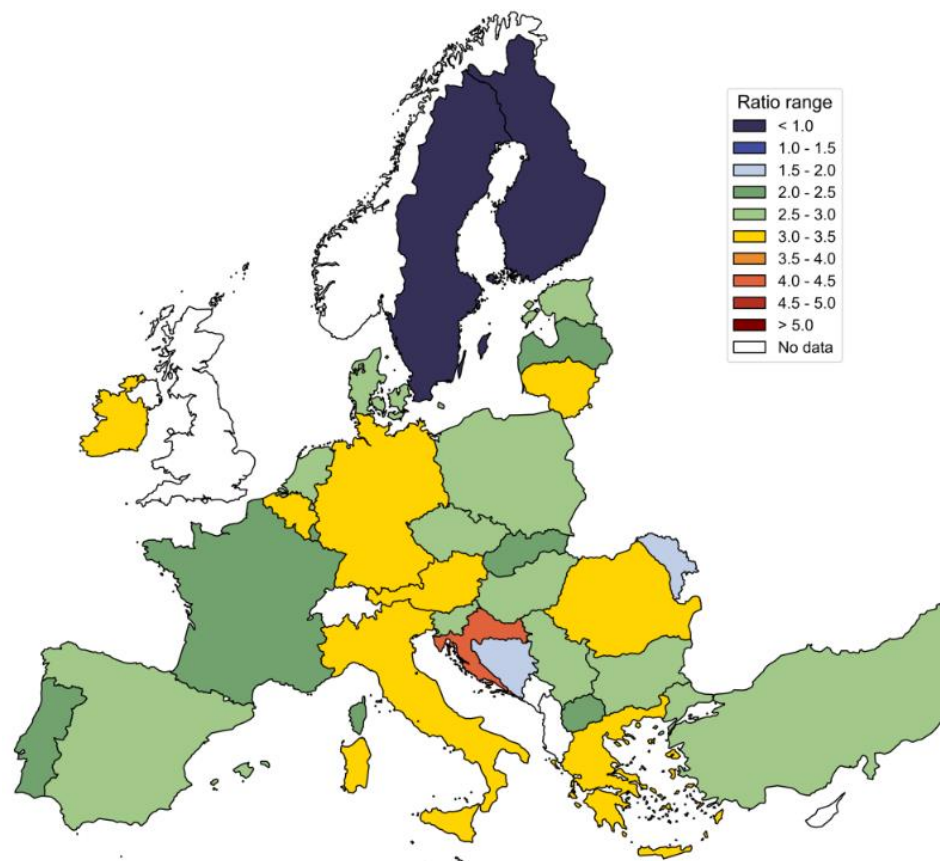


Figure 4. Electricity-to-gas price ratio for industrial end users in Europe (EHPA 2025a).

This ratio provides an excellent overall picture of the prevailing situation. In Figure 5 below, the effect of the ratio between electricity and natural gas prices on the number of heat pump investments in European households is shown. Although the situation is positive and the ratio low in the Nordic countries, the price of electricity in many Central and Southern European countries is more than double, or even triple, compared to the price of natural gas. While heat pump technology is continually developing on a large scale, this fact nevertheless slows down investment decisions in many industrial companies. In several countries, the ratio has decreased significantly in recent years and has increased interest in steam generating heat pump systems on a large scale. Despite this, the final investment decisions are also hindered by other factors, such as the limited number of practical applications for the technology and the lack of standardised solutions. (Arpagaus & Bertsch n.d.)

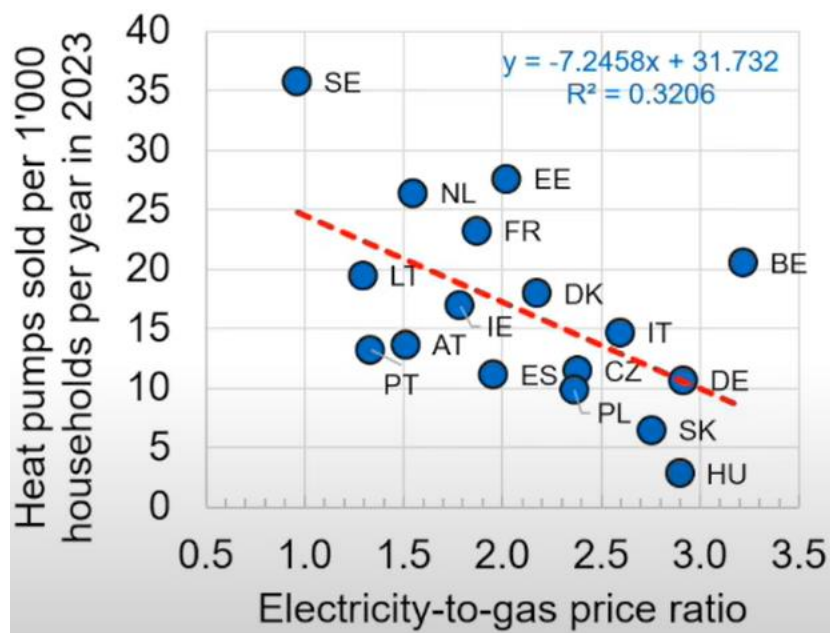


Figure 5. Number of heat pumps sold as a function of electricity-to-gas price ratio in different European countries (EHPA 2025b).

The same trend is visible in households, in industry, and in the energy production sector. Figure 5 shows that in almost all countries, the number of heat pumps sold decreases as the ratio of electricity-to-natural gas prices increases. The most significant exception is Belgium, where despite the high ratio, an unusually large number of heat pumps has been sold. The number of large-scale heat pumps used in district heating production in relation to the ratio of electricity and natural gas prices is illustrated in the diagram below (Figure 6).

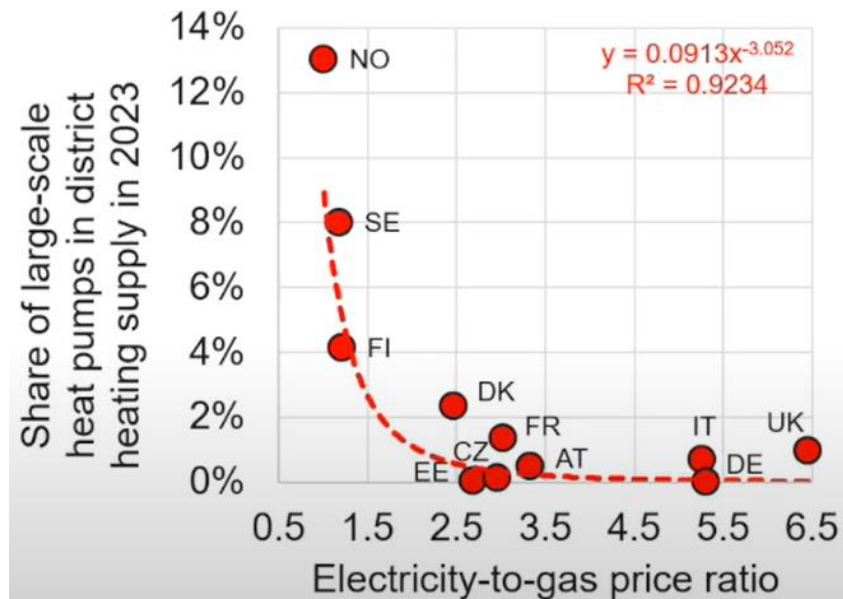


Figure 6. The share of large-scale heat pumps in district heating production as a function of electricity-to-gas price ratio in different European countries (EHPA 2025b).

As in Figure 5, the curve in Figure 6 decreases following the same principle. Compared to 2010, the utilisation of waste heat in district heating production in Finland has increased fivefold. The capacity of electrified district heating production is estimated to double from current levels by 2030. (Finnish Energy 2025) In both Finland and the other Nordic countries, the low price of electricity has been a major incentive for making heat pump investments. On the other hand, higher natural gas prices compared to many other European countries have equally contributed to the electrification of district heating in the Nordic region. (Eurostat 2025)

### 3 Steam generating heat pump

A steam-generating heat pump refers to a high-temperature heat pump used to produce steam for a process or other application. This section reviews the operation of a steam-generating heat pump, refrigerants suitable for high temperatures, and systems intended for increasing steam pressure. The definition of a high-temperature heat pump is not entirely unambiguous. In general, studies classify high-temperature heat pumps as those whose heat sinks are above 100 °C and below 160 °C. (Arpagaus et al. 2018; Ma et al. 2024) Waste heat sources in industry are almost always below 100 °C, and their temperatures typically fall within the 30–70 °C range (Arpagaus et al. 2018). This thesis examines high-temperature heat pumps that, through different configurations, produce +160 °C steam (6,18 bar). This section presents the vapour compression refrigeration cycle and discusses the operation of a steam-generating heat pump and the refrigerants suitable for high-temperature heat pumps. In addition, this section introduces the system by which the temperature and pressure of the steam produced by the heat pump can be increased to the desired level.

#### 3.1 Heat pump theory

The operation of a heat pump is based on a vapour compression refrigeration cycle known as the reverse Carnot cycle. Through this process, heat is transferred from a lower temperature to a higher temperature. This is made possible by the work done on the process. In the refrigeration cycle, heat is absorbed and released by the refrigerant circulating in the process. (Jiang et al. 2024; Kaappola et al. 2023) A simple process always includes at least the following components: evaporator, compressor, condenser, and expansion device. Figure 7 presents the components and principle of a closed refrigeration cycle. In the centre of the figure, a pressure–enthalpy diagram of the refrigerant is also shown, which is commonly used to illustrate refrigeration processes. To the left of the black curve the refrigerant is in liquid phase, within the curve the refrigerant is in the two-phase region (part vapour, part liquid), and to the right side is the region of superheated vapour.

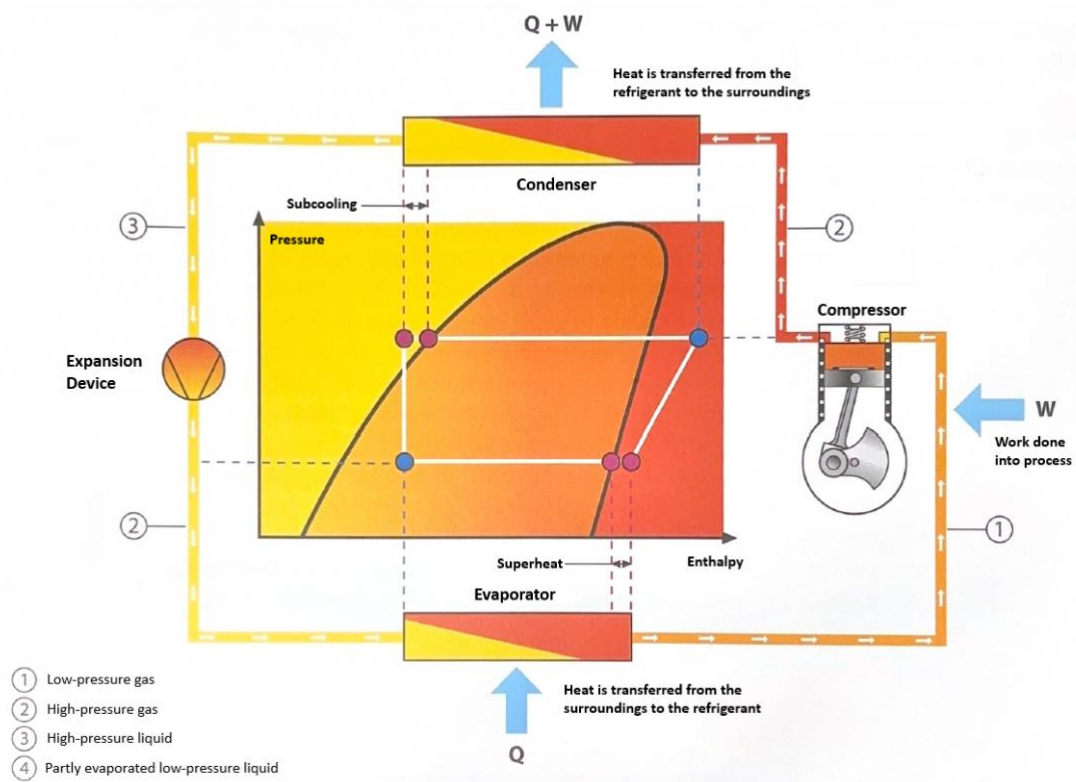


Figure 7. Refrigeration cycle (Adapted from Kaappola et al. 2023).

In a so-called subcritical cycle, the refrigerant evaporates in the evaporator (2–1) as it absorbs energy from the environment, i.e., from the heat source. The refrigerant always becomes slightly superheated in the evaporator to ensure that it does not enter the two-phase region (inside the curve) after compression, which would allow liquid droplets to enter the compressor. The required degree of superheating depends on the properties of the refrigerant used. After this, the refrigerant is directed to the compressor, where it is compressed (1–2). Compression increases the pressure of the refrigerant and thereby also its temperature. After the compressor, the refrigerant is directed to the condenser, where it condenses back into liquid while releasing heat energy to the environment, i.e., to the heat sink (2–3). In or after the condenser, the refrigerant is typically subcooled. After the condenser, the liquid refrigerant is directed to the expansion device, where its pressure and temperature decrease. This causes partial evaporation of the refrigerant. After the expansion device, the refrigerant begins the cycle again. In a subcritical process, the entire cycle occurs below the critical point of the refrigerant. (Kaappola et al. 2023)

The Carnot cycle represents an ideal cycle. The efficiency of the Carnot cycle is theoretical and represents the maximum possible efficiency that a cycle can achieve. The Carnot cycle

has no losses and is thermodynamically reversible. (Herold et al. 2016) The efficiency of a refrigeration cycle is described by its coefficient of performance, also known as COP (Coefficient of Performance). The theoretical COP value of a heat pump can be determined when the temperatures of its heat source and heat sink are known. The theoretical COP of heat production can be calculated using the following equation:

$$COP_{Carnot} = \frac{T_H}{T_H - T_C} \quad (1)$$

, where  $T_H$  is the temperature of the heat sink [K] and  $T_C$  the temperature of the heat source [K].

The actual COP value of a heat pump indicates how much heating or cooling is produced relative to the electrical energy consumed by the heat pump's compressor. When producing heat, the COP value is calculated using the following formula:

$$COP = \frac{Q_H}{P_C} \quad (2)$$

, where  $Q_H$  is the heat output delivered to the heat sink [kW] and  $P_C$  the compressor power input [kW]. (HPTTCP 2023)

The actual COP value is significantly lower than the theoretical Carnot COP, as shown earlier in figure 2. This is due to thermal and pressure losses occurring in the piping, compressor, and heat exchangers.

### 3.2 Working principle of a steam generating heat pump

In this thesis, the operation of a steam-generating heat pump is based on a closed-cycle compression heat pump, and MVR-system working in an open cycle attached to the lower cycle. In principle, the components of the closed-cycle compression heat pump remain the same as in other industrial heat pumps. Water can be evaporated either in the condenser of the heat pump, which in this case is referred to as the steam generator, or in a separate steam separator, where the pressure of the hot water coming from the condenser is reduced when entering the vessel, causing the water to partially evaporate and form saturated steam. The remaining liquid water settles at the bottom of the vessel and mixes with the make-up water supplied to the process. With a steam separator, only saturated steam can be produced,

whereas with a steam generator functioning as the condenser of the heat pump, it is possible to reach the region of slightly superheated steam. (Klute et al. 2024)

A welded plate & shell heat exchanger is typically used as the steam generator. This type of heat exchanger combines the pressure and temperature resistance of a shell-and-tube heat exchanger with the excellent heat transfer characteristics of a plate heat exchanger. (Vahterus 2020) In a plate & shell heat exchanger, a welded circular plate pack made of round heat transfer plates is placed inside a cylindrical steel shell. The circular shape of the heat transfer plates and the shell provides excellent durability. (Beckedorff 2022) In the case of a heat pump, the refrigerant condenses on the plate side of the heat exchanger and transfers heat to the shell-side medium, which in this case is water. On the shell side, the water evaporates as it flows between the plate packs. Figure 8 illustrates the flows occurring inside the plate & shell heat exchanger. The refrigerant flows downward inside the plate pack, while the evaporating water on the shell side flows upward.

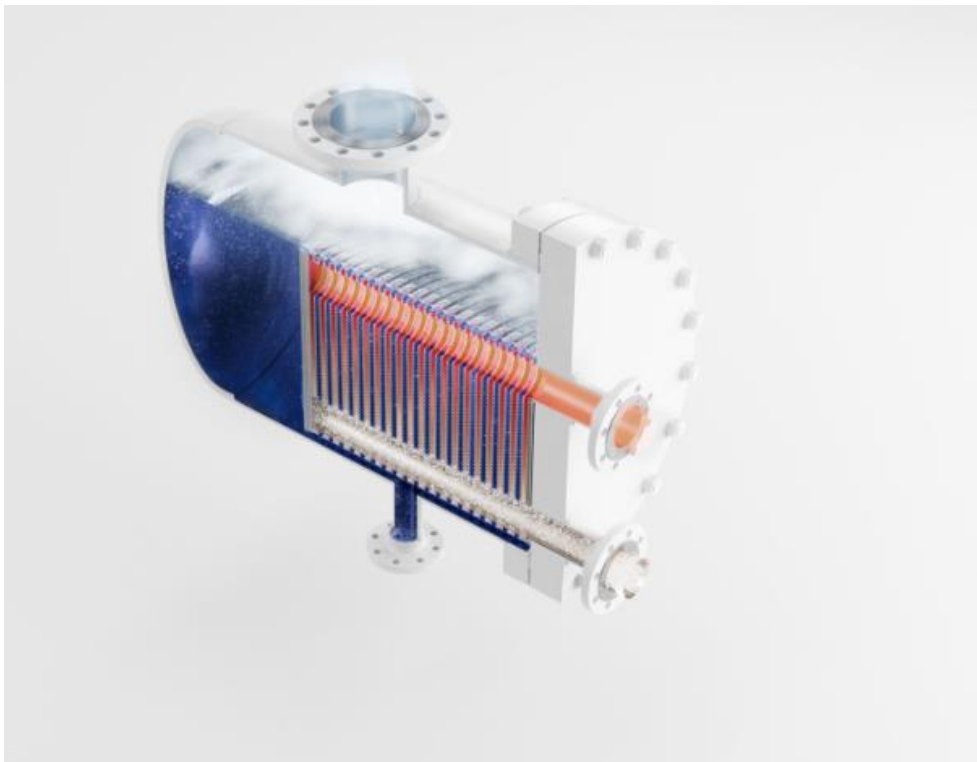


Figure 8. Flows of media in a plate & shell heat exchanger (Vahterus n.d.).

The phenomenon occurring in a steam separator is called flash evaporation. In this phenomenon, hot water is directed to a pressure reduction valve, where its pressure decreases

significantly. As results of the pressure drop, the liquid water expands to 2-phase area, causing some of the liquid to evaporate. For the flash effect to occur, the temperature of the water entering the pressure reduction valve must be at least a few degrees higher than the saturation temperature corresponding to the pressure prevailing in the steam separator. The operating principle of a flash steam separator is shown in Figure 9. Steam separators and flash evaporation in general have been utilised, among other applications, in geothermal energy production, the chemical industry, and alumina production. (Mansour et al. 2019)

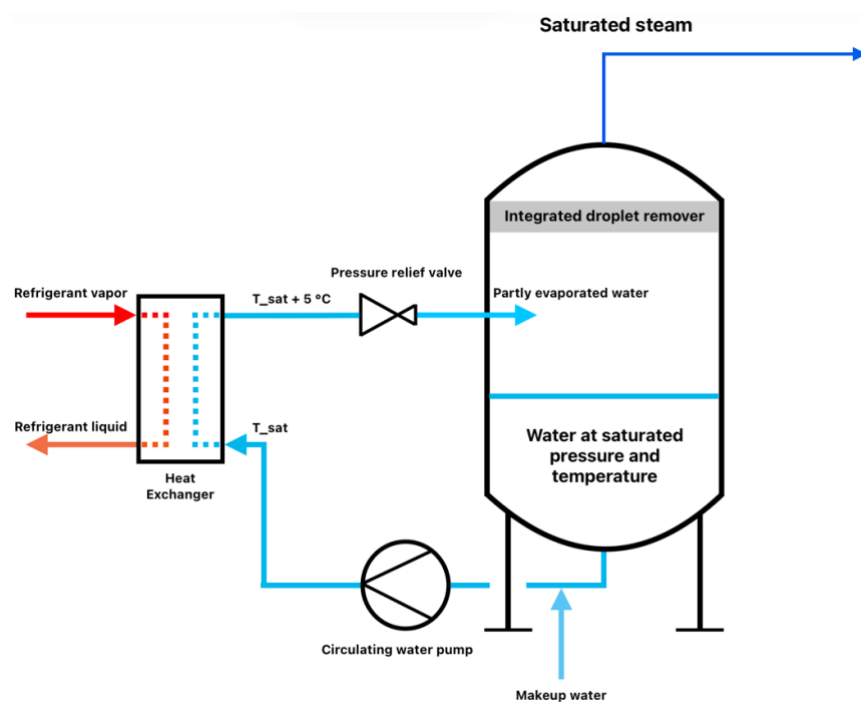


Figure 9. Flash tank working principle.

In the figure above, the steam separator configuration is implemented so that a circulation pump circulates water through the heat exchanger, where the water temperature increases by 5 degrees above the temperature of the steam separator vessel. In the upper part of the steam separator, an integrated droplet separator is installed to prevent liquid water from entering the steam piping and other systems. Makeup water is added into the system with a mass flow corresponding to the steam generation rate.

### 3.3 Refrigerants

Refrigerants are used as the medium for transferring heat in the refrigeration process. The use of refrigerants is based on their phase changes. A refrigerant evaporates from liquid to vapour when it absorbs heat from the environment and condenses from vapour to liquid when it releases heat to the environment. This phase change absorbs and releases large amounts of energy, enabling the transfer of even high heat loads with relatively small mass flow in the refrigeration process. (Kaappola et al. 2023) This section discusses different refrigerants and their suitability for high-temperature heat pumps.

Hydrocarbons in which hydrogen atoms have been synthetically replaced by certain halogen molecules are referred to as halogenated hydrocarbons. These refrigerants are classified in legislation according to their halogen molecules. The groups of synthetic refrigerants include Perfluorocarbons (PFC), Chlorofluorocarbons (CFC), Hydrochlorofluorocarbons (HCFC), Hydrofluorocarbons (HFC), Hydrofluoroolefins (HFO), and Hydrochlorofluoroolefins (HCFO). In addition to these, there are the so-called natural refrigerants, which include ordinary hydrocarbons (HC) and inorganic refrigerants such as water, carbon dioxide, and ammonia. Hydrocarbons belong to the group of flammable refrigerants, and therefore their safe use requires certain special arrangements when used in heat pumps. However, they are believed to achieve the same or even better efficiency than synthetic refrigerants. Ammonia, in turn, is a toxic and mildly flammable refrigerant. (Arpagaus et al. 2018; Jiang et al. 2022; Kaappola et al. 2023)

The EU's new F-gas regulation restricts the use of refrigerants with a high GWP value, meaning a strong global warming impact. (EU-2024/573) In addition, the Montreal Protocol from the 1980s restricted the use of refrigerants with a high ODP value, i.e., those causing ozone depletion. (Arpagaus et al. 2018) These restrictions significantly reduce the use of synthetic refrigerants. Considering the future of synthetic refrigerants, only HFO and HCFO refrigerants will remain in use, as the others generally have high GWP values. The GWP values of hydrocarbons and other natural refrigerants are very low. As a result, their use will increase as heat pumps using natural refrigerants replace heat pumps using high GWP refrigerants.

### 3.3.1 The working fluid of a steam generating heat pump

For a steam-generating heat pump, the selection of the correct refrigerant is a critical part of the heat pump design. The cooling and heating provided by a heat pump are based on the refrigerant cycle, in which the refrigerant evaporates and condenses as it absorbs heat from the environment and releases it. The refrigerant is therefore central to the operation of the heat pump. Choosing the right refrigerant is important, as it largely determines how efficiently and with what performance the heat pump can operate. The selection of a refrigerant mainly considers three factors: performance, safety, and environmental impact. (Moran et al. 2014)

Ma et al. 2024 and Sulaiman et al. 2023 list the key criteria for refrigerants used in high-temperature heat pumps. These include a low GWP value, an ODP value of zero, a high critical temperature, and low pressure at high temperatures, as well as excellent thermodynamic properties. Thermodynamic properties generally refer to good volumetric heating capacity, low vapour specific volume, high thermal conductivity, high latent heat, and high vapour density. In addition, the refrigerant should tolerate thermal decomposition well when mixed with the lubricant, i.e., compressor oil. The criteria in numerous studies also mention non-toxicity and low flammability. Furthermore, a sufficiently high evaporation pressure prevents air from entering the system when the equipment is stopped. (Arpagaus et al. 2018; Ma et al. 2024) Table 3 presents the properties of refrigerants suitable for high-temperature heat pumps.

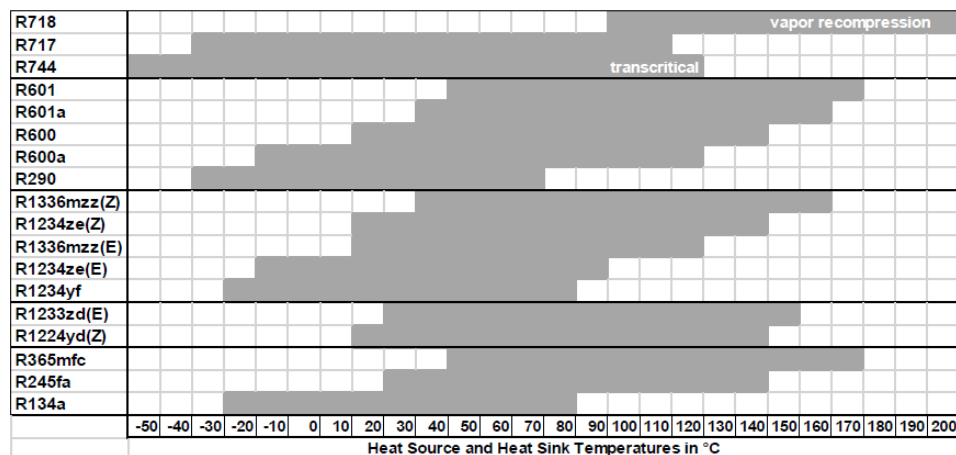
The selection of a refrigerant is largely based on the magnitude of the heat sink temperature. In this way, the most suitable refrigerant for the process can be identified to achieve the highest possible efficiency. For a subcritical refrigerant cycle, the limiting factor is the critical temperature of the refrigerant. To achieve the best possible COP value and to ensure that the refrigerant cycle remains subcritical, the condensation temperature of the refrigerant must be approximately 10–15 °C lower than the critical temperature of the refrigerant. A low refrigerant pressure in the heat pump system is desired, as it reduces the compressor pressure ratio and therefore the compressor work. In addition, a low refrigerant pressure places less mechanical stress on the equipment. (Arpagaus et al. 2018) However, if the evaporation pressure is too close to atmospheric pressure, there is a risk that air and

consequently moisture may enter the piping of the heat pump. The operating temperature ranges of different refrigerants are presented in Table 4.

Table 3. Properties of refrigerants suitable for high-temperature heat pumps (HPTTCP 2023).

Type	Working fluid	Description	$T_{crit}$ (°C)	$p_{crit}$ (bar)	ODP (-)	GWP (-)	SG
Natural	R-718	Water	373.9	220.6	0	0	A1
	R-717	Ammonia	132.3	113.3	0	0	B2L
	R-744	Carbon dioxide	31.0	73.8	0	1	A1
HC	R-601	n-Pentane	196.6	33.7	0	5	A3
	R-601a	Isopentane	187.8	33.8	0	4	A3
	R-600	n-Butane	152.0	38.0	0	4	A3
	R-600a	Isobutane	134.7	36.3	0	3	A3
	R-290	Propane	96.7	42.5	0	3	A3
HFO	R-1336mzz(Z)	1,1,1,4,4,4-Hexafluoro-2-butene	171.3	29.0	0	2	A1
	R-1234ze(Z)	cis-1,3,3,3-Tetrafluoro-1-propene	150.1	35.3	0	<1	A2L
	R-1336mzz(E)	trans-1,1,1,4,4,4,-Hexafluoro-2-butene	130.4	27.8	0	18	A1
	R-1234ze(E)	trans-1,3,3,3-Tetrafluoro-1-propene	109.4	36.4	0	<1	A2L
	R-1234yf	2,3,3,3-Tetrafluoro-1-propene	94.7	33.8	0	<1	A2L
HCFO	R-1233zd(E)	1-chloro-3,3,3-Trifluoro-propene	166.5	36.2	0.00034	1	A1
	R-1224yd(Z)	1-chloro-2,3,3,3-Tetrafluoro-propene	155.5	33.3	0.00012	<1	A1
HFC	R-365mfc	1,1,1,3,3-Pentafluorobutane	186.9	32.7	0	804	A2
	R-245fa	1,1,2,2,3-Pentafluoropropane	154.0	36.5	0	858	B1
	R-134a	1,1,1,2-Tetrafluoroethane	101.1	40.6	0	1'300	A1

Table 4. Operating temperatures of different refrigerants (HPTTCP 2023).



In a study conducted by Sulaiman et al. (2022), low-GWP refrigerants were compared in a theoretical assessment. The purpose of the assessment was to determine the performance and thermodynamic properties of different refrigerants when using a high-temperature heat pump with a single-stage configuration and an internal heat exchanger. A mathematical

analysis was developed in the study, enabling the determination of various performance parameters for each refrigerant. The heat source and heat sink temperatures ranged between 60 and 70 °C and 90 and 140 °C. The study revealed the suitability of pentane (R601), R1233zd(E), and R1336mzz(Z) as replacements for the higher-GWP HFC refrigerant R245fa.

Arpagaus et al. (2018) also developed a model of a single-stage system with an internal heat exchanger, enabling a comparison of the thermodynamic properties of different refrigerants. Both synthetic and natural refrigerants (hydrocarbons) were included in the analysis. The refrigerants were divided into two categories according to their minimum degree of superheat, ensuring that each refrigerant could operate under optimal conditions. Figure 10 shows the COP values of the investigated refrigerants as a function of condensation temperature (graph a) and volumetric heating capacity (VHC) as a function of condensation temperature (graph b). In the analysis, the evaporation and condensation temperatures varied, but the temperature lift remained constant (70 K).

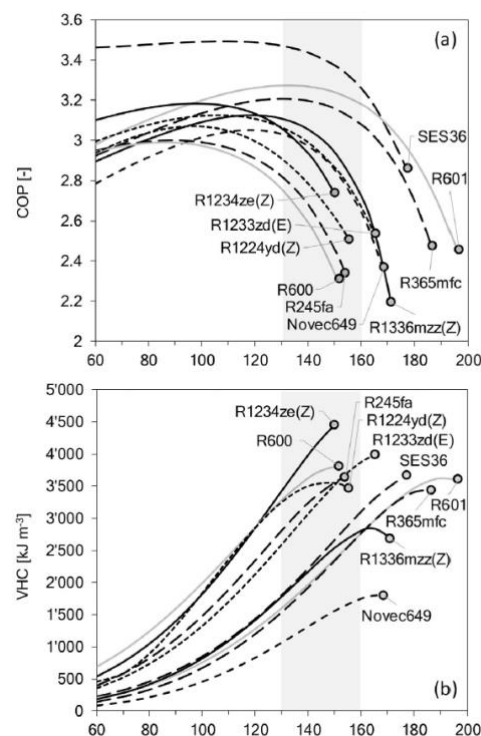


Figure 10. Different refrigerants' COP and volumetric heating capacity as a function of condensing temperature (Arpagaus et al. 2018).

From the graphs, it can be seen how the COP values gradually decrease as the condensation temperature increases. This is because, at higher condensation temperatures, the temperature lift increases, and therefore the COP value decreases as shown in Figure 7. An interesting finding in graph a is that the best COP value for many refrigerants is achieved between 120 and 140 °C condensation temperatures. For example, R1233zd(E) achieves its highest COP at approximately 120 °C, whereas pentane achieves its highest COP at around 135 °C. In terms of volumetric heating capacity, butane, R1234ze(Z), and R1233zd(E) show superiority compared to the other refrigerants.

### 3.3.2 Refrigerants selected for the technical comparison

This section presents the refrigerants that are used in the profitability assessment. The detailed operating values of the refrigerants are presented in Section 4.1.1. In addition to the synthetic refrigerants R1234ze(E) and R1233zd(E), isobutane (R600a) was included in the profitability assessment in order to also incorporate a natural refrigerant. Moreover, R600a is a refrigerant available in the sizing software provided by Compressor Manufacturer 2, meaning it is a commonly used refrigerant.

R1234ze(E) belongs to the synthetic HFO refrigerants and is a mildly flammable A2L-category refrigerant. It has a low GWP value, a critical temperature of 109.4 °C and a critical pressure of 36.4 bar. Due to its similar operating range and favourable thermodynamic performance, R1234ze(E) has been considered one of the potential candidates to replace the higher-GWP HFC refrigerant R134a. (Al-Sayyab et al. 2022; Arpagaus et al. 2018) R1234ze(E) has also been used by Calefa in several applications for heat pumps producing district heating.

R1233zd(E) belongs to the HFCO refrigerants and is a synthetic A1-category refrigerant with a low GWP value. Its critical temperature is 166.5 °C and its critical pressure is 36.2 bar. Its normal boiling point is 18 °C, and its vapour pressure at 20 °C is only 1.079 bar, which may cause air ingress into the refrigerant circuit during standstill conditions (Arpagaus et al. 2018). As an HFCO refrigerant, its ODP value is not zero (0.00034), but its atmospheric lifetime before decomposition is short, and therefore its impact is minimal. (Zini et al. 2024) R1233zd(E) has excellent thermodynamic properties, combining high

volumetric heating capacity with an excellent COP. For high-temperature heat pumps, R1233zd(E) has been reported to be an exceptionally suitable refrigerant. (Sulaiman et al. 2022; Jeßberger et al. 2024)

Isobutane (R600a) is a hydrocarbon and classified as an A3-category highly flammable refrigerant. It has a low GWP value and an ODP value of zero, and its critical temperature and pressure are 134.7 °C and 36.3 bar. The normal boiling point of isobutane is -11.75 °C. Isobutane is widely used in household refrigeration appliances such as refrigerators. As a hydrocarbon, its high flammability may limit its applicability in larger-scale systems (Jiang et al. 2022). However, isobutane is well suited to high-temperature heat pumps due to its properties (Bamigbetan et al. 2018). As shown in Table 4, isobutane can be used to produce heat up to approximately 120 °C. In this work, however, its use is limited to below 100 °C.

Water (R718) is an inexpensive and globally highly available refrigerant. It is non-toxic and non-flammable. Water is chemically stable, and its thermodynamic properties—such as a critical temperature of +374 °C and a critical pressure of 221.3 bar—enable high temperature levels. Water also has a high latent heat, which gives it a greater potential compared to many other refrigerants when high temperature levels are required. For this reason, it functions as an excellent medium for heat transfer. The pressure of water remains moderate even at high temperature levels, and when water is used, the refrigerant process remains subcritical. Challenges associated with the use of water include its low molar mass, large vapour specific volume, and high polytropic exponent (pressure increases rapidly when the liquid is compressed). These properties lead to exceptionally high pressure ratios, large volumetric flow rates, and high discharge temperatures on the compressor outlet side. In addition, the natural boiling point of water is +100 °C, meaning that for lower temperature applications the pressure must be kept below atmospheric pressure. (Arpagaus et al. 2018; Ma et al. 2024; Zini et al. 2024)

A compression heat pump using water as the refrigerant is typically an open-loop system in which low-pressure steam is upgraded to high-pressure steam. Suitable systems for this purpose include large turbocompressors operating at temperatures above +100 °C. (Jiang et al. 2024) This steam pressure increase is known as MVR (Mechanical Vapour Recompression). MVR technology is discussed in more detail in Section 3.4.

### 3.3.3 The future of refrigerants

For synthetic refrigerants with low GWP values (HFO and HFCO), concern has been raised over their classification as so-called PFAS compounds (per- and polyfluoroalkyl substances). The degradation product of these compounds, TFA (trifluoroacetic acid), is a persistent substance, and its accumulation in nature and water bodies has been identified as potentially harmful. The European Chemicals Agency (ECHA) may in the future restrict the use of PFAS compounds through the REACH regulation. This may mean that synthetic refrigerants are entirely phased out in the future. Heat pump manufacturers must stay up to date on refrigerant-related restrictions to avoid unexpected bans. (ECHA 2024)

As synthetic refrigerants may at some point be subject to restrictions, the future of refrigerants appears to be shifting increasingly towards the use of natural - and consequently also flammable - refrigerants (Zini et al. 2024). Their use, however, requires additional safety measures and special requirements for the equipment. Overall, hydrocarbons are highly suitable for many industrial applications, and with careful consideration of risk factors, their safe use is possible. (Vavilov 2025) A useful guide on the use of flammable refrigerants in heat pumps is Rath (2019). The guide discusses a wide range of service and maintenance procedures for refrigeration equipment, as well as methods for mitigating risks in such tasks.

## 3.4 Mechanical vapor recompression

Mechanical Vapor Recompression (MVR) refers to the mechanical compression of steam, operating in an open cycle. The working fluid is process steam in the gaseous phase, whose pressure and temperature are increased using a compressor. Compression can be carried out with several types of steam compressors, such as radial, roots, or screw compressors (Ma et al. 2024). Typically, large radial compressors are used, operating at relatively low pressure ratios to compensate for the low density of steam (Arpagaus et al. 2018). Different manufacturers may use slightly different terminology for their equipment, which is why in this thesis the term *radial compressor* is used interchangeably with *radial blower* when referring to MVR technology. Figure 11 illustrates the operating principle of a radial compressor.

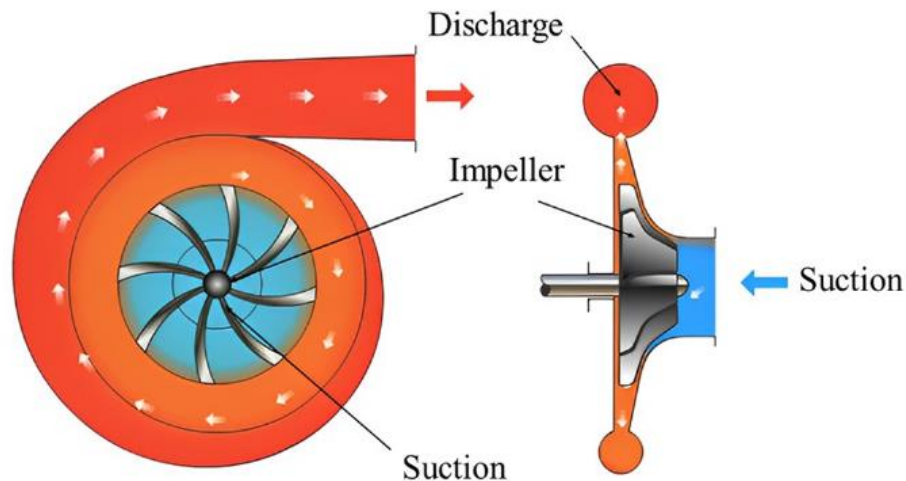


Figure 11. Working principle of a radial MVR compressor (Ma et al. 2024).

The arrows in the figure indicate the flow direction of the working fluid (steam). A radial compressor is a kinetic compressor where the blades of a rapidly rotating impeller increase the velocity and pressure of incoming steam. When the steam collides with the diffuser section, its pressure and temperature rise. The higher-pressure steam then flows into the volute (Ma et al. 2024). Due to losses occurring within the compressor, the steam always becomes slightly superheated, resulting in a higher actual temperature rise. To avoid equipment damage caused by excessive discharge temperatures, spray water injection is commonly used to remove superheat. Water injected into the compressor suction vaporises upon contact with the incoming steam, thereby cooling it and decreasing the required work for compression. Spray water injection also increases the steam mass flow rate, improving the compressor's heat output (Klute et al. 2024; Tolvanen 2018). The use of spray water requires careful optimisation to determine the correct injection rate. Excessive injection reduces the overall pressure ratio and isentropic efficiency of the compressor (Ma et al. 2024). Figure 12 illustrates three compressions steps of steam in a log  $p$ - $h$  diagram, where spray water is used in each stage to remove superheat.

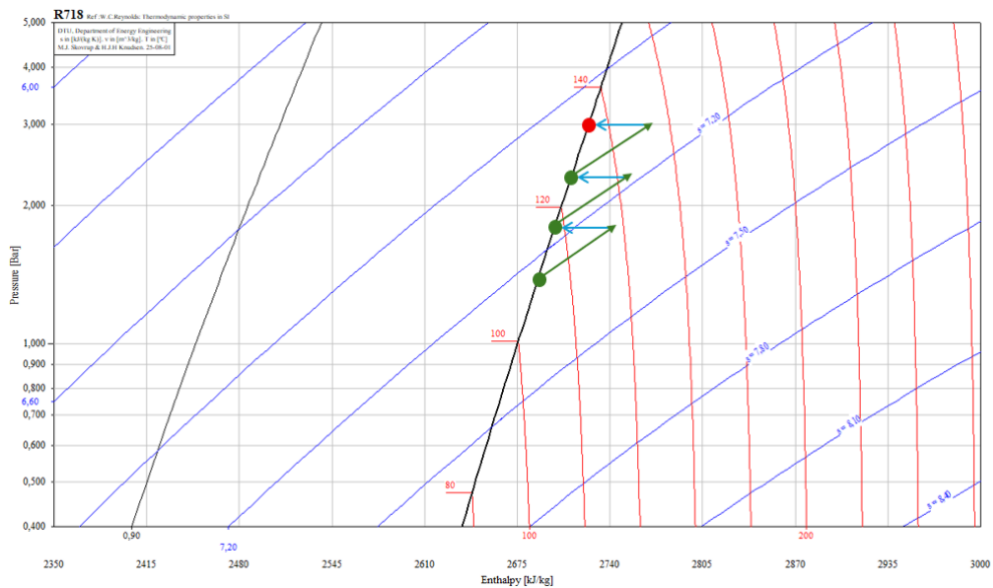


Figure 12. 3-stage compression of steam in a log p,h -chart.

The green arrows represent the compression process, during which both the pressure and temperature of steam rise. In this example, steam becomes superheated by approximately 20 °C at each stage, which is removed with spray water (blue arrows). With spray cooling, the process can operate close to the saturated vapour line. In the example, the steam pressure is raised from 1,43 bar to 3 bar.

The design of radial compressors must also consider the materials used. To avoid corrosion of impeller blades and other components, material selection is highly important. Various materials are used in impellers, such as stainless steel, titanium, molybdenum, and carbon fibre (Ma et al. 2024). Because the equipment is sensitive to water droplets, one manufacturer specifies that droplets of 1 mm diameter or larger must be prevented from entering the compressor. Klute et al. (2024, p. 9) similarly states: *“For some MVR designs, it must also be ensured that no water droplets remain in the generated steam from the closed-loop HP.”*

Tolvanen (2018) performed a modelling study on the influence of spray cooling on the operation of MVR blowers using fluid dynamics. The study concluded that spray cooling improves the efficiency of radial blowers. Since the spray is injected as liquid water, some droplets inevitably enter the blower. In the simulation model, droplet sizes ranged from 500 µm to 1.5 µm. To achieve saturated steam, droplets sized 10–50 µm were found to perform best and integrated smoothly into the steam flow. Based on the findings, it can be assumed

that manufacturer-installed spray systems never exceed 1 mm droplet size and therefore do not pose a risk to the equipment.

A roots compressor works by directing low-pressure steam into a suction chamber, where a pair of rotating rotors compress the steam to higher temperature and pressure (Figure 13) (Ma et al. 2024). After compression, the steam at elevated pressure is discharged via the discharge chamber. The roots compressor is a displacement compressor based on reducing the volume of the working chamber. Advantages of roots compressors include low vibration, dynamic balance, and simple design. Additionally, the compressor is not highly sensitive to water droplets (Bin et al. 2018; Ma et al. 2024). Some manufacturers also highlight their low noise levels (Atlas Copco n.d.). The disadvantages include limited volumetric capacity, low pressure ratio, and relatively poor compression efficiency. Thus, the compressor is unsuitable for higher-pressure applications (Bin et al. 2018).

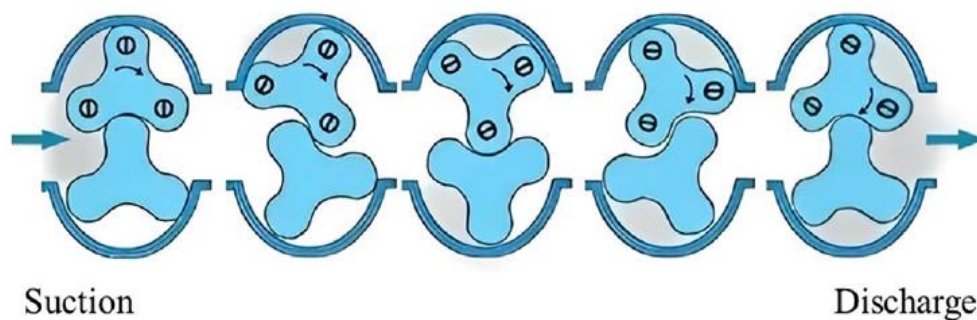


Figure 13. Working principle of a multi-stage roots-compressor (Ma et al. 2024)

A screw compressor is a displacement compressor in which steam is compressed between two intermeshing rotating screws. Steam enters the compressor from the suction side. In a twin-screw compressor, one rotor is driven by an electric motor. As the screws rotate, the trapped volume between them decreases, raising the pressure and temperature of the steam to the desired level (Ma et al. 2024). The operating principle of a screw compressor is shown in Figure 14. Advantages include high pressure ratio capability, durability, stability, and good controllability. However, the volumetric capacity is relatively small, which limits its use to small and medium-sized steam systems (Bin et al. 2018). As with roots compressors, steam becomes significantly superheated when compressed, so spray cooling or an equivalent technique is required to control the final discharge temperature (Ma et al. 2024).

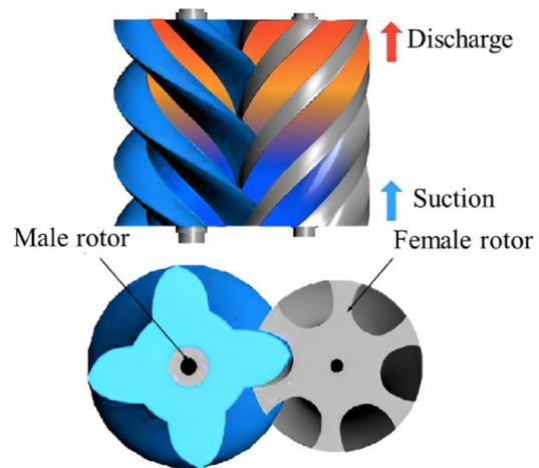


Figure 14. Working principle of a screw compressor (Ma et al. 2024).

In this thesis, the economic feasibility analysis is conducted for a system where the MVR technology is based **on a** radial compressor.

## 4 Technical comparison

In the economic feasibility analysis, two different steam production configurations were compared, along with the steam production capacities they can achieve. Based on the steam production capacities, it is possible to estimate the maximum mass flow rate of evaporated water that the system can produce. From this, the total number of heat pumps required in the system can be determined. In addition, the COP values of the configurations were compared to evaluate in which situation each steam production configuration would be the most advantageous.

In the analysis, the heat pump system was set to produce steam at a maximum of 6,18 bar and a temperature of +160 °C. For each power level, the steam production configurations were set to generate steam mass flows of 2500 (1,43 and 3,62 bar(a)) and 5000 kg/h (6,18 bar(a)). The heat pump sizing was carried out using the design software of two different compressor manufacturers. The calculations also utilised the Danfoss Coolselector 2 software, which enabled the determination of refrigerant enthalpies at various points in the process. The enthalpies of steam were calculated using water vapour h,s tables.

### 4.1 Heat pump connections

For the steam production configurations, vacuum steam at +85 °C was generated using three different heat pump setups, each producing vacuum steam into a separate steam separator vessel, as shown in Figure 9. In the values calculated with Manufacturer 1's sizing software, an economizer configuration was applied for both single-stage and two-stage screw compressors due to the varying evaporation temperatures. Using the second Manufacturer's sizing software, the performance values of the isobutane heat pump were calculated when operating with a typical hydrocarbon-compatible configuration: a single-stage screw compressor equipped with an internal heat exchanger (IHX). Some hydrocarbons require an internal heat exchanger because they need a higher degree of superheating to prevent liquid refrigerant from entering the compressor.

The economizer configuration and the internal heat exchanger configuration are presented in Figure 15. The figures also illustrate the refrigerant cycle on a log p–h diagram for each configuration. In both Manufacturers' sizing software, the largest available compressor was selected for this analysis.

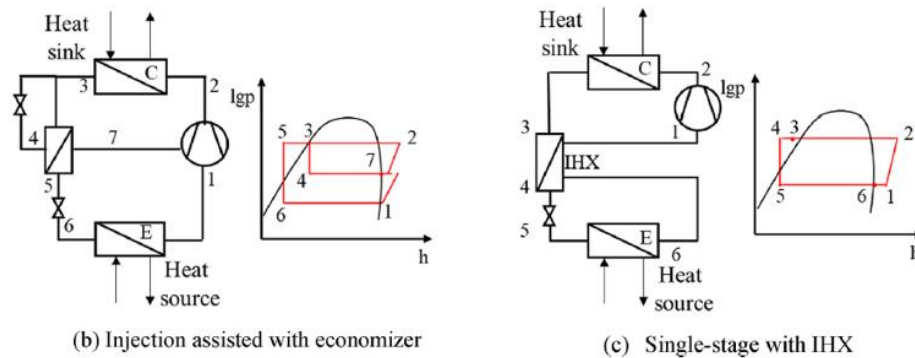


Figure 15. Single-stage economizer and IHX connections (Jiang et al. 2022).

#### 4.1.1 Operating values of refrigerants

The selection of refrigerants was guided primarily by the temperature levels chosen for the techno-economic assessment. In the direct steam-generation configuration, the heat pump's condenser (steam generator) together with mechanical vapor recompression (MVR) first produce steam at +110 °C (1,43 bar(a)), after which the MVR unit compresses the vapor to 3,62 and 6,18 bar(a). When examining the applicable temperature ranges of different refrigerants, the HFCO refrigerant R1233zd(E) was found to be well suited for this purpose. When generating +110 °C steam, the corresponding refrigerant condensing temperature settles at approximately +120 °C. As shown earlier in Figure 10, R1233zd(E) achieves its highest efficiency at this condensing temperature and is therefore highly suitable for generating low-pressure steam directly in the steam generator. As a synthetic refrigerant it is also non-flammable, which makes it a safe and practical choice for this analysis.

The initial parameters selected for the steam-generator configuration are presented in Table 5. The table lists compressor type, degree of superheat, and compressor pressure ratio  $\epsilon$ , which was calculated from the ratio of the pressures corresponding to the evaporating and

condensing temperatures. Subcooling was set to 0 °C in all calculations so that only the heat delivered for steam production is considered when evaluating condenser performance.

Table 5. The initial values for R1233zd(E) in direct steam generation.

Refrigerant	R1233z d(E)	R1233z d(E)	R1233z d(E)	R1233z d(E)	R1233z d(E)	R1233z d(E)	R1233z d(E)	R1233z d(E)
Compressor (380V-3-60Hz)	1-stage screw	1-stage screw	1-stage screw	1-stage screw	1-stage screw	1-stage screw	1-stage screw	1-stage screw
Economiser	Yes	Yes	Yes	Yes	Yes	Yes	Yes	Yes
Evaporation temperature [°C]	40	45	50	55	60	65	70	75
Condensating temperature [°C]	120	120	120	120	120	120	120	120
Useful superheat [°C]	10	10	10	10	10	10	10	10
Pressure ratio $\epsilon$	7,31	6,25	5,37	4,64	4,03	3,52	3,08	2,71

For the steam-separator configuration, three refrigerants were selected that can produce +85 °C steam under sub-atmospheric pressure. First, R1234ze(E) is a familiar refrigerant for Calefa and has been used in many large-scale heat-pump installations, such as district-heating production. R600a (isobutane) is a natural refrigerant which, due to its excellent operational range, is expected to become a potential replacement for R1234ze(E) in the future. R1233zd(E) was also included due to its suitable operating range for low-pressure steam generation. The input values used for each refrigerant in this configuration are presented in Tables 6, 7, and 8. The condensing temperature was set to +94 °C so that, considering condenser approach temperatures, the water entering the expansion valve would be approximately +90 °C.

Table 6. The initial values for R1234ze(E) in flash steam generation.

Refrigerant	R1234ze(E)	R1234ze(E)	R1234ze(E)	R1234ze(E)	R1234ze(E)	R1234ze(E)	R1234ze(E)
Compressor (380V-3-60Hz)	2-stage screw	2-stage screw	2-stage screw	1-stage screw	1-stage screw	1-stage screw	1-stage screw
Economiser	Yes	Yes	Yes	Yes	Yes	Yes	Yes
Evaporation temperature [°C]	15	20	25	31	35	40	45
Condensating temperature [°C]	94	94	94	94	94	94	94
Useful superheat [°C]	10	10	10	10	10	10	10
Pressure ratio $\epsilon$	7,37	6,28	5,39	4,51	4,02	3,50	3,06

Table 7. The initial values for R600a in flash steam generation.

Refrigerant	R600a	R600a	R600a	R600a	R600a	R600a	R600a	R600a
Compressor (380V-3-60Hz)	1-stage screw	1-stage screw	1-stage screw	1-stage screw	1-stage screw	1-stage screw	1-stage screw	1-stage screw
Economiser	No (IHx)	No (IHx)	No (IHx)	No (IHx)	No (IHx)	No (IHx)	No (IHx)	No (IHx)
Evaporation temperature [°C]	15	20	25	31	35	40	45	50
Condensating temperature [°C]	94	94	94	94	94	94	94	94
Useful superheat [°C]	15	15	15	15	15	10	10	10
Pressure ratio $\epsilon$	6,85	5,87	5,06	4,38	3,82	3,34	2,94	2,59

Table 8. The initial values for R1233zd(E) in flash steam generation.

Refrigerant	R1233zd(E)	R1233zd(E)	R1233zd(E)
Compressor (380V-3-60Hz)	1-stage screw	1-stage screw	1-stage screw
Economiser	Yes	Yes	Yes
Evaporation temperature [°C]	50	55	60
Condensating temperature [°C]	94	94	94
Useful superheat [°C]	10	10	10
Pressure ratio $\epsilon$	3,11	2,69	2,34

Due to its thermodynamic properties, butane requires a higher degree of superheat at low evaporating temperatures. This prevents the refrigerant from entering the two-phase region after compression. For the synthetic refrigerants, a 10 °C superheat was used for all configurations. In the two-stage screw-compressor configuration of R1234ze(E), the pressure ratio is divided between two rotors, which maintains a higher isentropic efficiency.

## 4.2 Calculations

This section represents the calculation procedure beginning with the closed cycle heat pump calculations and continuing further to the steam generating connections. A visual representation of the calculation process can be seen in the calculation flow chart (figure 16) below.

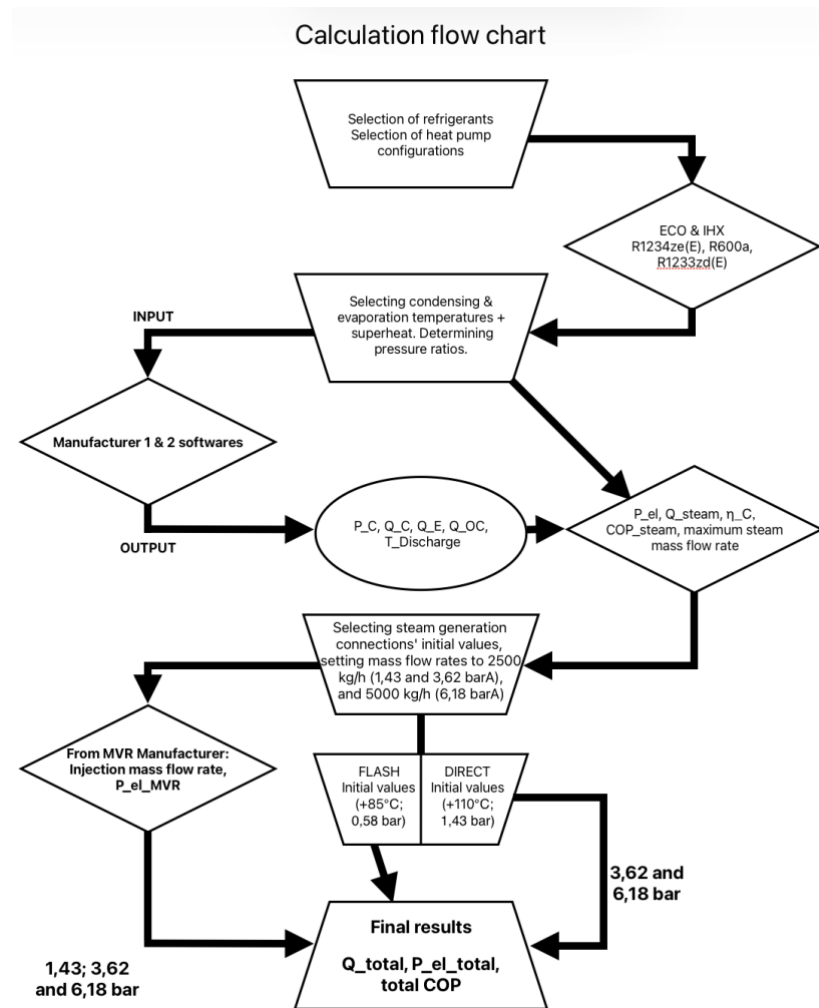


Figure 16. Calculation flow chart for the technical comparison

In the calculations, the steam production capacity and COP of the heat pump were determined solely based on condenser output. Any heat recovered from oil cooling was therefore subtracted from the total heating capacity reported by the manufacturer's selection software. Similarly, the COP was calculated using only the heat delivered for steam production. The electrical power consumption provided by the software was corrected using a frequency-converter adjustment factor, as frequency converters introduce a small electrical loss into the system. Thus, the actual electrical power input was calculated as follows:

$$P_{elHP} = \tau P_C \quad (3)$$

, where  $P_{el_{HP}}$  is the actual electrical input power of the heat pump [kW],  $P_C$  is the compressor power reported by the selection software [kW], and  $\tau$  is the frequency-converter correction factor. A value of  $\tau = 1,03$  was used in this work.

The steam-production COP of the heat pump was calculated using the following equation:

$$COP_{steam} = \frac{Q_{steam}}{P_{el_{HP}}} \quad (4)$$

, where  $Q_{steam} = Q_C - Q_{OC}$  is the heat pump's steam-production capacity [kW].

In the calculations, the compressor's isentropic efficiency was also examined, using the equation below. Isentropic compression refers to ideal compression of the refrigerant without losses, during which entropy remains constant:

$$\eta_c = \frac{h_{2s} - h_1}{h_2 - h_1} \quad (5)$$

, where  $\eta_c$  is the compressor isentropic efficiency,  $h_1$  the refrigerant enthalpy before the compressor [kJ/kg],  $h_2$  the refrigerant enthalpy after the compressor [kJ/kg], and  $h_{2s}$  the refrigerant enthalpy after isentropic compression [kJ/kg].

The enthalpies were calculated once the pressures corresponding to the refrigerant's evaporation and condensation temperatures, the refrigerant's superheat before the compressor, and the discharge temperature were known. The discharge temperature was obtained from the Manufacturer 1 selection software. In the case of R600a, the enthalpy after compression was calculated using the compressor power equation, because the selection software did not provide the discharge temperature for the compression process:

$$P_C = \dot{m}(h_2 - h_1) \quad (6)$$

where  $\dot{m}$  is the refrigerant mass flow through the compressor [kg/s], solving for  $h_2$  gives:

$$h_2 = h_1 + \frac{P_C}{\dot{m}} \quad (7)$$

The refrigerant enthalpy after isentropic compression  $h_{2s}$  was determined once the refrigerant entropy before compression and the refrigerant pressure after compression were known.

#### 4.2.1 Flash tank vs. Steam generator

In the flash tank, the temperature is +85 °C and the water in the vessel is saturated (0.579 bar). The +90 °C circulation water coming from the condenser is directed through a pressure-reducing valve, where part of it vaporises as the pressure is reduced to the flash tank pressure. It was assumed that there are no losses due to blowdown etc. occurring in the flash tank. The fraction of water that vaporises from the circulating stream can be calculated using the following equation:

$$\dot{m}_{flash} h_{flash} = \dot{m}_{circ} h_{circ} + \dot{m}_{steam} h_{steam} \quad (8)$$

where  $\dot{m}_{flash}$  and  $h_{flash}$  are the mass flow rate [kg/s] and enthalpy [kJ/kg] of the water flowing through the pressure-reducing valve,  $\dot{m}_{circ}$  and  $h_{circ}$  are the mass flow rate [kg/s] and enthalpy [kJ/kg] of the circulating water, and  $\dot{m}_{steam}$  and  $h_{steam}$  are the mass flow rate [kg/s] and enthalpy [kJ/kg] of the vaporised water. From the mass balance:

$$\dot{m}_{flash} = \dot{m}_{circ} + \dot{m}_{steam} \quad (9)$$

Substituting this into the previous equation and solving for the ratio of vaporized water and circulating water we obtain:

$$\frac{\dot{m}_{steam}}{\dot{m}_{circ}} = \frac{h_{flash} - h_{circ}}{h_{steam} - h_{flash}} \quad (10)$$

By substituting the enthalpy values into the equation, the fraction of vaporized water from circulating water is:

$$x = \frac{\dot{m}_{steam}}{\dot{m}_{circ}} = \frac{377 \frac{kJ}{kg} - 355,9 \frac{kJ}{kg}}{2651,3 \frac{kJ}{kg} - 377 \frac{kJ}{kg}} * 100\% = 0,93\% \quad (11)$$

Here, x is the ratio between the mass of vaporized and liquid water. The circulating water mass flow rate can be solved from the condenser power equation:

$$Q_{condenser} = \dot{m}_{circ} c_p \Delta T \quad (12)$$

, where  $c_p$  is the specific heat capacity of water [kJ/kgK] and  $\Delta T$  is the temperature difference across the condenser [K]. Solving for the mass flow rate gives:

$$\dot{m}_{circ} = \frac{Q_{condenser}}{c_p \Delta T} \quad (13)$$

From the circulating mass flow rate, the mass flow of vaporized water can be solved:

$$\dot{m}_{steam} = x \dot{m}_{circ} \quad (14)$$

In this work, the electricity consumption of the possible vacuum pump in the flash tank is not considered, as it is assumed significantly smaller than the total electricity consumption of the system. The circulation pump power can be calculated using the following equation:

$$P_{circ} = \dot{m}_{circ} \Delta h_{circ} \quad (15)$$

, where  $P_{circ}$  is the circulation-pump power [kW], and  $\Delta h_{circ}$  the enthalpy change in the water across the pump [kJ/kg].

For the low-pressure steam-generation analysis, the total electrical power of the heat pump + flash-tank system is obtained by adding the circulation-pump power to the heat pump's electrical power:

$$P_{el_{flash}} = P_{el_{HP}} + P_{el_{circ}} \quad (16)$$

The enthalpy change is obtained from:

$$\Delta h_{circ} = \frac{v_{in} \Delta p}{\eta_{circ}} \quad (17)$$

, where  $v_{in}$  is the specific volume of water before the circulation pump [m<sup>3</sup>/kg],  $\Delta p$  the pressure increase created by the pump [kPa], and  $\eta_{circ}$  the pump efficiency. A typical efficiency of 80 % is used. The required pressure increase must be high enough to prevent boiling of the water in the condenser. A pressure difference of 100 kPa was selected in this case to cover the pressure losses in the heat exchanger and piping. The water parameters at the different state points are presented in Table 9.

Table 9. Water parameters for flash tank connection in difference process points

	Circulating water	Flash water	Steam
Temperature [°C]	85	90	85
Pressure [bar]	0,579	1,079	0,579
Enthalpy [kJ/kg]	355,9	377,0	2651,3
Specific heat capacity [kJ/kgK]	4,2	4,2	4,2
Specific volume [m <sup>3</sup> /kg]	0,001033	0,001036	2,829

It was assumed for the steam generator that the condensate entering the generator is at 100 °C. In the steam generator, the water is first heated to 110 °C, after which it evaporates. The steam is directed through a droplet separator located at the top of the steam generator before entering the steam pipe, ensuring that the resulting steam is as saturated as possible. The water parameters for the steam-generator configuration are presented in Table 10.

Table 10. Water parameters for direct steam generation

	Condensate	Saturated steam
Temperature [°C]	100	110
Pressure [bar]	1,43	1,43
Enthalpy [kJ/kg]	419,1	2691,1

For the steam-generator configuration, the maximum steam production rate of the heat pump can be calculated using the steam generator's heat output with the following equation:

$$\dot{m}_{steam} = \frac{Q_{steam}}{h_{steam} - h_{condensate}} \quad (18)$$

, where  $h_{steam}$  is the enthalpy of saturated steam [kJ/kg], and  $h_{condensate}$  is the enthalpy of the condensate [kJ/kg]. This makes it possible to determine how many heat pumps are required in the system to achieve the desired steam flow rate.

$$n_{HP} = \frac{\dot{m}_{system}}{\dot{m}_{steam}} \quad (19)$$

, where  $n_{HP}$  is the number of heat pumps, and  $\dot{m}_{system}$  is the total steam mass flow selected for the system [kg/h].

#### 4.2.2 MVR after steam generation

For the analysis, two different steam-system mass flow rates were selected (2500, 5000) and three different pressure levels (1,43 bar; 3,62 bar; 6,18 bar). For the highest pressure level (6,18 bar; +160 °C), the analysis was conducted using steam flows of 5000 kg/h. This is due to the MVR system requirement that, at higher pressure levels, the blower needs a higher flow rate to prevent the steam volumetric flow from becoming too low. The mass flow rate 2500 kg/h leads to a too low volumetric flow in 6,18 bar steam production.

The MVR system includes injection water in each blower stage. Therefore, the total thermal capacity of the system increases, as the system mass flow increases due to the MVR blowers according to the following equation:

$$\dot{m}_{total} = \dot{m}_{steam} + \dot{m}_{inj} \quad (20)$$

, where  $\dot{m}_{total}$  is the steam mass flow after the MVR blowers [kg/s], and  $\dot{m}_{inj}$  is the amount of injection water from the MVR system [kg/s].

The total thermal capacity of the system can be calculated when the steam mass flow after the MVR system and the steam enthalpy after the MVR system are known:

$$Q_{total} = \dot{m}_{total}(h_{steam\,final} - h_{condensate}) \quad (21)$$

where  $Q_{total}$  is the total steam capacity of the system [kW],  $h_{steam\,final}$  is the steam enthalpy after the MVR blowers, and  $h_{condensate}$  is the condensate enthalpy according to the connection (flash or direct generation).

The total electrical consumption of the system is calculated for both the flash-steam configuration and the steam generator configuration as follows:

$$P_{el_{tot}} = nP_{el_{flash}} + P_{el_{MVR}} \quad (22)$$

and

$$P_{el_{tot}} = nP_{el_{HP}} + P_{el_{MVR}} \quad (23)$$

where  $P_{el_{tot}}$  is the total electrical consumption of the system [kW], and  $P_{el_{MVR}}$  is the electrical consumption of the MVR blowers [kW]. The overall system coefficient of performance is then obtained as:

$$COP_{total} = \frac{Q_{total}}{P_{el_{tot}}} \quad (24)$$

## 5 Results and analysis of technical comparison

This section first reviews the calculation results for the performance of the steam heat pumps, followed by the performance of the different systems when MVR blowers are utilized resulting in various pressure levels. After this, the performance, total steam generation output with the COP values are compared between the systems.

### 5.1 Steam generating heat pumps

Steam production was assessed using two different steam configurations and three different heat pump configurations (single- and two-stage screw configurations with an economizer, as well as a single-stage screw with an internal heat exchanger). In the first case, 110 °C steam was produced directly in the heat pump condenser, i.e., in the steam generator. The input values for this analysis were presented in Table 5. In the second case, 85 °C low-pressure steam was produced using the input values listed in Tables 6, 7, and 8.

Table 11 presents the calculated results for 110 °C steam production, including the heat pump evaporator capacity, condenser steam capacity, compressor power consumption, steam-production COP, and the maximum achievable steam production rate. Tables 12, 13, and 14 present the corresponding results for 85 °C steam production. The tables also show the compressors' isentropic efficiencies and compression ratios. The evaporating temperatures for each case are also shown.

Table 11. The calculation results for R1233zd(E) in direct steam

	Refrigerant : R1233zd(E)							
Compressor (380V-3-60Hz)	1-stage screw	1-stage screw	1-stage screw	1-stage screw	1-stage screw	1-stage screw	1-stage screw	1-stage screw
Evaporation temperature [°C]	40	45	50	55	60	65	70	75
Evaporator power [kW]	503	601	719	857	1015	1194	1396	1624
Steam power [kW]	<b>811</b>	<b>917</b>	<b>1043</b>	<b>1187</b>	<b>1349</b>	<b>1537</b>	<b>1745</b>	<b>1978</b>
Heat pump electric power [kW]	343	348	353	359	365	371	377	383
Steam COP	<b>2,37</b>	<b>2,64</b>	<b>2,96</b>	<b>3,31</b>	<b>3,70</b>	<b>4,15</b>	<b>4,63</b>	<b>5,16</b>
Max. steam generating capacity [kg/h]	<b>1285</b>	<b>1453</b>	<b>1653</b>	<b>1881</b>	<b>2138</b>	<b>2435</b>	<b>2766</b>	<b>3134</b>
Pressure ratio	7,31	6,25	5,37	4,64	4,03	3,52	3,08	2,71
Isentropic efficiency [%]	57,40	60,63	64,33	67,59	69,90	71,09	71,43	71,48

Table 12. The calculation results for R1234ze(E) in flash steam generation

	Refrigerant : R1234ze(E)						
Compressor (380V-3-60Hz)	2-stage screw	2-stage screw	2-stage screw	1-stage screw	1-stage screw	1-stage screw	1-stage screw
Evaporation temperature [°C]	15	20	25	31	35	40	45
Evaporator power [kW]	469	540	618	1191	1374	1637	1922
Steam power [kW]	<b>697</b>	<b>776</b>	<b>860</b>	<b>1549</b>	<b>1736</b>	<b>2000</b>	<b>2272</b>
Heat pump electric power [kW]	302	317	336	588	605	630	658
Steam COP	<b>2,31</b>	<b>2,44</b>	<b>2,56</b>	<b>2,64</b>	<b>2,87</b>	<b>3,17</b>	<b>3,46</b>
Max. steam generating capacity [kg/h]	<b>1098</b>	<b>1223</b>	<b>1355</b>	<b>2426</b>	<b>2735</b>	<b>3151</b>	<b>3580</b>
Pressure ratio	7,37	6,28	5,39	4,51	4,02	3,50	3,06
Isentropic efficiency [%]	77,26	77,58	76,72	70,52	71,16	71,08	70,53

Table 13. The calculation results for R600a in flash steam generation

	Refrigerant : R600a							
Compressor (380V-3-60Hz)	1-stage screw	1-stage screw	1-stage screw	1-stage screw	1-stage screw	1-stage screw	1-stage screw	1-stage screw
Evaporation temperature [°C]	15	20	25	31	35	40	45	50
Evaporator power [kW]	332	402	489	592	716	845	1009	1193
Steam power [kW]	<b>595</b>	<b>669</b>	<b>762</b>	<b>873</b>	<b>1006</b>	<b>1144</b>	<b>1319</b>	<b>1512</b>
Heat pump electric power [kW]	274	280	287	295	305	315	327	338
Steam COP	<b>2,17</b>	<b>2,39</b>	<b>2,66</b>	<b>2,96</b>	<b>3,30</b>	<b>3,63</b>	<b>4,04</b>	<b>4,47</b>
Max. steam generating capacity [kg/h]	<b>938</b>	<b>1055</b>	<b>1201</b>	<b>1376</b>	<b>1585</b>	<b>1803</b>	<b>2078</b>	<b>2383</b>
Pressure ratio	6,85	5,87	5,06	4,38	3,82	3,34	2,94	2,59
Isentropic efficiency [%]	61,66	64,93	67,38	70,08	71,19	70,62	70,19	68,37

Table 14. The calculation results for R1233zd(E) in flash steam generation

	Refrigerant : R1233zd(E)		
Compressor (380V-3-60Hz)	1-stage screw	1-stage screw	1-stage screw
Evaporation temperature [°C]	50	55	60
Evaporator power [kW]	989	1168	1368
Steam power [kW]	<b>1173</b>	<b>1369</b>	<b>1575</b>
Heat pump electric power [kW]	233	241	249
Steam COP	<b>5,04</b>	<b>5,69</b>	<b>6,34</b>
Max. steam generating capacity [kg/h]	<b>1848</b>	<b>2157</b>	<b>2481</b>
Pressure ratio	3,11	2,69	2,34
Isentropic efficiency [%]	72,70	71,48	68,60

Based on the results, the highest steam production capacity (2272 kW) is achieved when using the low-pressure steam system and a single-stage screw compressor with R1234ze(E) as the refrigerant and an evaporating temperature of 45 °C. In this case, the steam-production COP is 3.46 and the maximum achievable steam production is 3580 kg/h. A similar steam production level is reached with direct steam production at +110 °C when the evaporating temperature is 75 °C. In that case, the system's steam output is 1978 kW, and the COP is 5,16. The highest COP value (6,34) is achieved with the single-stage screw compressor using R1233zd(E) when producing low-pressure steam with an evaporating temperature of 60 °C. However, the system's steam output is lower (1575 kW) and the maximum steam flow is 2481 kg/h. The lower steam output of R1233zd(E) is due to the refrigerant's significantly lower density compared to R1234ze(E).

Isobutane outperforms R1234ze(E) in terms of COP values. The steam output is limited by the compressor of Manufacturer 2, which in this analysis is smaller than the corresponding one from Manufacturer 1. At the same evaporating temperature of 45 °C, isobutane achieves a COP of 4,04, which is 0,6 units higher than that of R1234ze(E). At the lowest evaporating

temperatures (15 and 20 °C), the two-stage screw compressor provides a slight advantage in COP and steam output compared to the single-stage isobutane compressor. At 25 °C, isobutane surpasses the two-stage screw compressor in both performance categories. At lower evaporating temperatures, the single-stage screw compressor suffers from reduced compression efficiency due to the higher compression ratio, giving the two-stage screw compressor better operating characteristics.

An important point of comparison is how the results differ between producing 110 °C steam and 85 °C steam when the heat pump operates at the same evaporating temperature. With R1234ze(E), at an evaporating temperature of 40 °C, a steam output of 2 MW is achieved, whereas at the same evaporating temperature and with 110 °C steam production, R1233zd(E) reaches only 811 kW. In the 45 °C case, R1234ze(E) reaches both the compressor's evaporating-temperature limit and its maximum capacity of 2272 kW. Under the same evaporating conditions, 110 °C steam production reaches 917 kW. In other words, when producing low-pressure steam, the Manufacturer 1's single-stage screw compressor achieves approximately 2,5 times the steam output at these evaporating temperatures. The COP of the low-pressure system is also about 1 unit higher in both cases at the same evaporating temperatures.

Regarding isentropic compression efficiencies, the two-stage screw compressor achieves the highest values. This is because the two-stage screw can operate with higher compression ratios, as the pressure increase is divided between two separate rotors. Thus, the two-stage screw compressor performs optimally when higher temperature lifts are required. For the single-stage screw compressors, the best isentropic compression efficiency is achieved when the compressor pressure ratio is approximately 3–4.

## 5.2 Total system performance (Steam generating heat pump + MVR)

The first systems examined were steam systems where the steam flow produced by the heat pumps was defined as 2500 kg/h. For this mass flow, low-pressure steam was produced using the MVR system at both 1,43 bar and 3,62 bar pressure levels. In the direct steam production case, 1,43 bar steam was boosted to 3,62 bar. Figure 17 shows the required number of heat pumps as a function of evaporating temperature for each refrigerant and steam production

configuration. The number of heat pumps is not an integer in all cases, but it enables accurately determining the system's electrical power at each operating point.

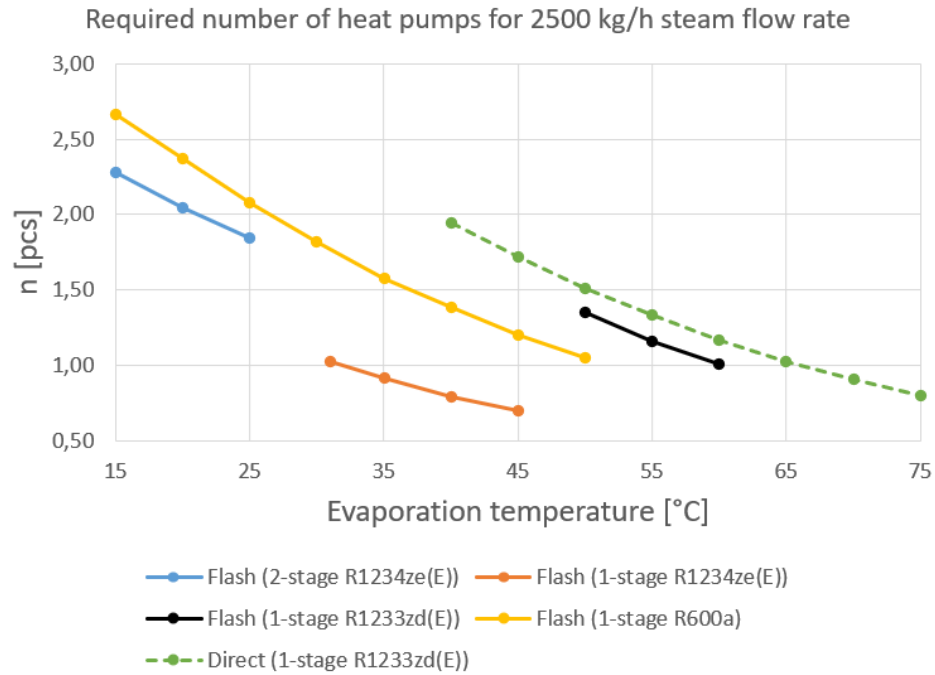


Figure 17. Required number of heat pumps of each system as a function of evaporation temperature

In addition to determining system electrical power, calculating the number of heat pumps is useful when estimating and comparing system costs. Differences in the number of heat pumps directly reflect differences in the heating capacities of individual units. However, this does not directly indicate the COP of the steam system, as the size differences between compressor manufacturers' compressors significantly influence the required quantity. The COP values for the 1,43 bar steam production case for each configuration are shown in Figure 18. Solid lines represent the flash-steam system + MVR blowers for different compressors, while the dashed line represents the direct steam production system.

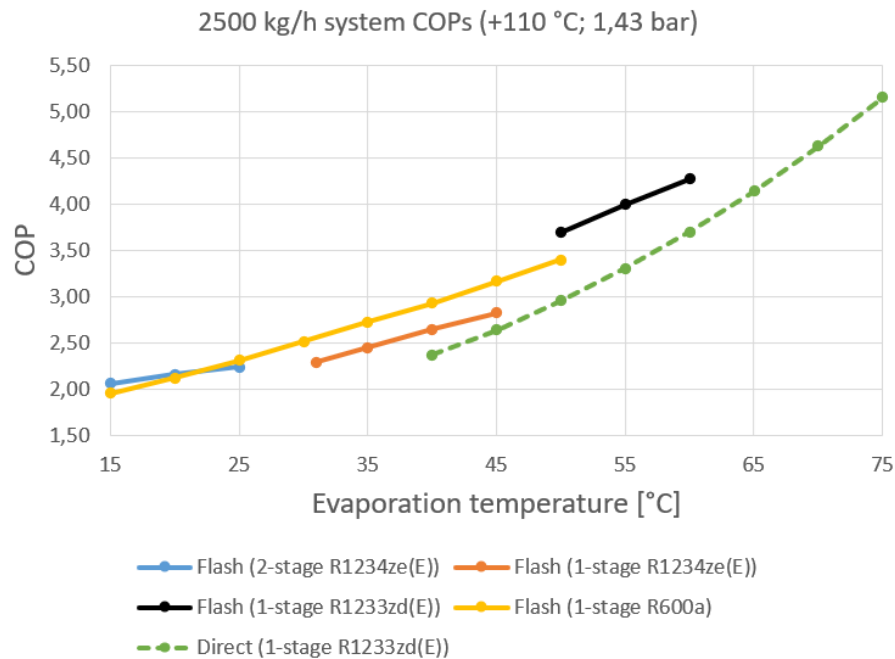


Figure 18. 1,43 bar, 2500 kg/h systems COP values as a function of evaporation temperatures

Based on the results, the highest COP in 110 °C steam production is achieved with the flash-steam system at high evaporating temperatures. This COP value is nearly one unit higher than the COP of direct steam production at the same evaporating temperatures. Overall, the best COP value is obtained with direct steam production when the evaporating temperature is 75 °C (COP  $\approx$  5,20). At lower evaporating temperatures, the flash-steam system achieves approximately 0,2–0,35 units (R1234ze(E)) and 0,50–0,65 units (R600a) higher COP compared to direct steam production. When comparing the performance of R1233zd(E) with flash and direct connections, the flash connection reaches even 0,75 higher COP than the direct connection at same evaporation temperatures, showing a clear performance advantage of the flash connection.

Considering the required number of heat pumps in Figure 17, the flash-steam configuration yields significantly better COP at lower evaporating temperatures with fewer heat pumps. Additionally, COP values of around 2,0 or slightly higher are obtained at the lower evaporating temperatures. No significant difference appears between single-stage and two-stage screw compressors regarding required heat-pump quantity. Figures 18 and 19 present the total system COP values when producing 3,62 bar steam (Figure 19) and 6,18 bar steam (Figure 20).

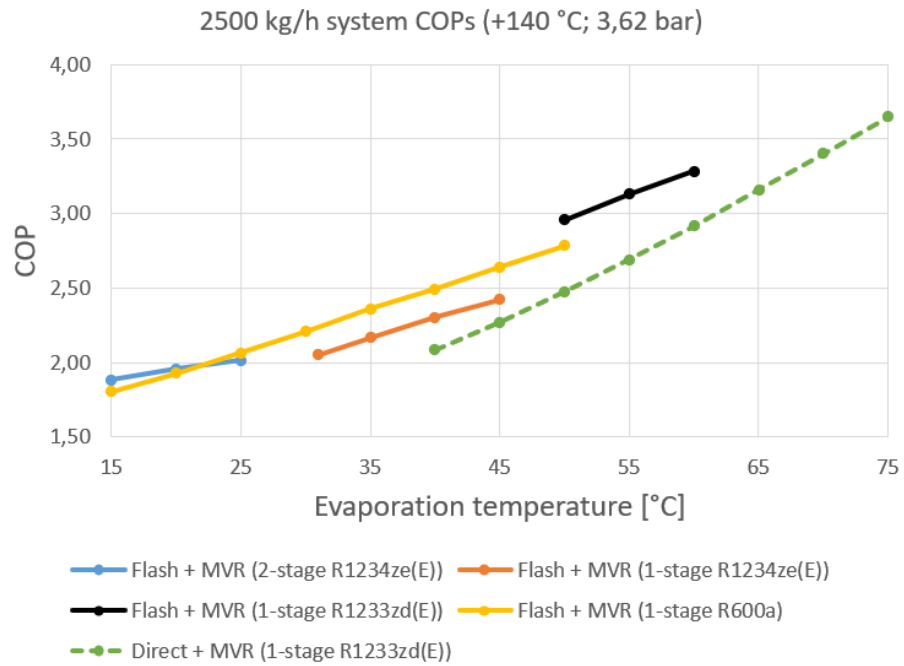


Figure 19. 3,62 bar, 2500 kg/h systems COP values as a function of evaporation temperatures

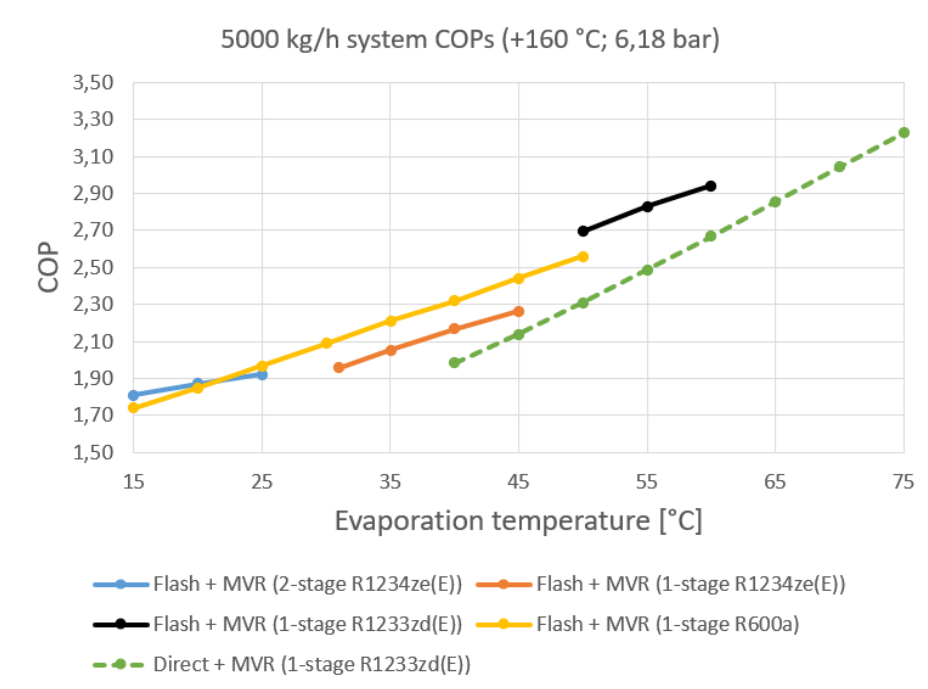


Figure 20. 6,18 bar, 5000 kg/h systems COP values as a function of evaporation temperatures

The decrease in COP values is expected since the MVR system's electrical consumption increases when additional blowers are needed to raise steam pressure to higher levels. Nevertheless, at evaporating temperatures of 40, 45, and 50 °C, COPs of approximately 2,0–2,7 are achieved for 3,62 bar steam production and 1,9–2,6 for 6,18 bar steam production. The highest COP values at these evaporating temperatures are achieved with the flash-steam configuration using the isobutane heat pump. It achieves approximately 0,2 higher COP compared to R1234ze(E), and 0,35 higher COP compared to the direct steam production + MVR configuration. At the lowest evaporating temperatures, the COP decreases roughly in between 1,7 and 1,9.

When increasing the pressure level using MVR, the overall system performance depends increasingly on the performance of the individual MVR stages. Since the isentropic efficiency of a radial compressor is typically higher than that of a screw compressor, the drop in COP between pressure levels is not as significant compared to direct steam generation using only a closed-cycle compression heat pump. In addition, when MVR is applied, the slope of the COP curves remains relatively linear, whereas in direct steam generation at 1,43 bar, the slope exhibits more exponential behaviour. This suggests that the performance of the direct steam generation system may be more sensitive to changes in evaporation temperature than that of the flash system. Moreover, when a larger share of the temperature lift is provided by the MVR cycle rather than the heat pump compressor, a system relying more on MVR achieves a higher COP. This is due to the increasing injection mass flow rate, which raises the thermal power, as well as the higher isentropic efficiency of the compression process.

## 6 Conclusions

As the decarbonization of industrial heat generation becomes increasingly viable with the development of high-temperature heat pump technologies, there is a clear need to assess different types of steam generation configurations. This thesis first presented the market potential of heat pumps in European countries, taking into account the critical factors affecting investment decision-making. These factors include available waste heat temperatures (mostly below 100 °C), available technologies for waste heat utilization in steam generation, and the electricity-to-gas price ratio.

Subsequently, the steam-generating heat pump was introduced through fundamental heat pump theory. The steam generation configurations used in the theoretical evaluation were then presented. The thesis also included a section discussing potential refrigerants for high-temperature heat pumps in detail, highlighting the current shift toward natural refrigerants. This shift is driven by implemented regulations such as the F-gas Regulation and forthcoming restrictions on synthetic refrigerants under REACH. To increase the steam pressure level, a separate MVR system is often utilized. Different types of MVR compressors were presented in Chapter 3.4, including desuperheating by water injection and the vapor compression process illustrated in a log p,h diagram.

The theoretical evaluation began with the selection of heat pump configurations and refrigerants. To ensure sufficient versatility, three refrigerants were selected: two synthetic refrigerants (R1234ze(E) and R1233zd(E)) and one hydrocarbon (R600a). For the synthetic refrigerants, 1- and 2-stage compression heat pumps equipped with an economizer were selected. For R600a, a single-stage cycle with an internal heat exchanger (IHX) was chosen. The selected evaporation temperatures ranged from 15 to 75 °C, while the condensing temperatures were 94 °C and 110 °C, depending on the steam generation configuration. The values were obtained from two different compressor manufacturers: one supplying 1- and 2-stage screw compressors for synthetic refrigerants, and the other supplying single-stage screw compressors also suitable for natural refrigerants. In all cases, the largest available compressor sizes were selected.

A central question in the design of steam-generating heat pump systems is which system configuration should be utilized and under what conditions. In this work, a comprehensive

comparison was conducted between two steam generation configurations. The first was an indirect steam generation method using a flash tank operating at vacuum pressure (0,579 bar), and the second was a direct steam generation method producing 1,43 bar steam using a plate & shell heat exchanger as the condenser of the closed-cycle heat pump. In both cases, the steam pressure was further increased to 3,62 and 6,18 bar.

In the flash configuration, the temperature lift achieved by the closed-cycle compression heat pump was not always as high as in the direct steam generation configuration. In this case, the temperature lift provided by the MVR system was greater than that provided by the heat pump itself, allowing the MVR system to supply a larger share of the required lift and resulting in improved overall system performance. Another advantage of the flash steam generation system was that the heating capacity of a single heat pump unit was significantly higher than in the direct steam generation configuration. The results indicate that, depending on the refrigerant, the COP values achieved with the flash configuration were 0,20 to 0,75 units higher than those of the direct steam generation configuration. This is a significant result and supports the use of steam compression as an advantageous technology when implementing high-temperature heat pumps and selecting the most suitable configuration. Water injection between MVR stages also increases the steam mass flow rate, thereby improving the heat output and overall COP.

This study compared two closed-cycle compression systems utilizing MVR as the upper cycle of the heat pump system. The results obtained for the MVR system are consistent with current research. However, comparative research on vacuum versus overpressure steam generation configurations remains limited and requires further investigation in terms of efficiency, investment cost, and technology readiness. This thesis did not consider the potential investment costs of a flash tank system, which is a significant factor when evaluating practical implementation. Additionally, the performance values for the heat pumps and MVR systems were derived from real manufacturers' software and provided data. Therefore, the obtained values may differ slightly from real-life performance. In practical applications, careful system integration may enable even better performance than that obtained in this study.

The results of this thesis can serve as a reference when implementing such systems in industrial steam processes. Further research should focus particularly on economic aspects, including OPEX and CAPEX considerations and their impact on system profitability. In

addition, expanding the comparison to include a broader range of refrigerants would be beneficial in identifying the most suitable configuration for different operating conditions.

## References

- Al-Sayyab A.K.S., Navarro-Esbrí, J. & Mota-Babiloni A., 2022. Energy, exergy, and environmental (3E) analysis of a compound ejector-heat pump with low GWP refrigerants for simultaneous data center cooling and district heating. *International Journal of Refrigeration*, 133, 61-72.
- Atlas Copco, n.d. Mechanical Vapor Recompression brochure. Available at: <https://www.atlascopco.com/fi-fi/vacuum-solutions/products/mechanical-vapor-recompression> (Accessed 31.7.2025)
- Arpagaus, C. & Bertsch, S. 2019. Experimental results of HFO/HFCO refrigerants in a laboratory scale HTHP with up to 150 C supply temperature.
- Arpagaus, C. & Bertsch, S. n.d. High-temperature heat pumps are on the rise – Why is their market uptake slow? [Column] Available at: <https://heatpumpingtechnologies.org/column-high-temperature-heat-pumps-are-on-the-rise-why-is-their-market-uptake-slow/> (Accessed 21.7.2025)
- Arpagaus, C., Bless, F., Uhlmann, M., Schiffmann, J. 2018. High temperature heat pumps: Market overview, state of art, research status, refrigerants, and application potentials. *Energy*, 152, 985 – 1010.
- Arpagaus, C. 2024. Webinar: 2024 High-temperature heat pumps update – with Dr Cordin Arpagaus. Published by the Australian Alliance for Energy Productivity. Available at: <https://www.youtube.com/watch?v=xJyxqYgHYBs> (Accessed 17.7.2025)
- Bamigbetan, O., Eikevik T.M., Neksa, P., Bantle, M. & Schlemminger, C., 2018. Theoretical analysis on suitable fluids for high temperature heat pumps up to 125 °C heat delivery. *International Journal of Refrigeration*, 92, 185-195.
- Beckedorff, L., da Silva, R.P.P., Martins, G.S.M., de Paiva K.V., Oliveira J.L.G. & Oliveira, A.A.M., 2022. Flow maldistribution and heat transfer characteristics in plate and shell heat exchangers. *International Journal of Heat and Mass Transfer*, 195, 123182.

Bin, H., Di, W. & Wang, R.Z. 2018. Water vapor compression and its various applications. *Renewable and Sustainable Energy Reviews*, 98, 92-107.

de Boer, R., Marina, A., Zühlsdorf, B., Arpagaus, C., Bantle, M., Wilk, V., Elmegaard, B., Corberán, J., & Benson, J. 2020. Strengthening Industrial Heat Pump Innovation: Decarbonizing Industrial Heat.

ECHA, 2024. Per- and polyfluoroalkyl substances (PFAS). Available at: <https://echa.europa.eu/hot-topics/perfluoroalkyl-chemicals-pfas> (Accessed 18.8.2025)

EHPA (European Heat Pump Association), 2025a. Electricity versus gas prices: what's the picture for industry? Available at: <https://www.ehpa.org/news-and-resources/news/electricity-versus-gas-prices-whats-the-picture-for-industry/> (Accessed: 17.7.2025)

EHPA (European Heat Pump Association), 2025b. The Road to Sustainable Industrial Heat: A Roundtable on the Future of Industrial Heat Pumps. [Webinar] Available at: [https://www.youtube.com/watch?v=9C\\_JWsyx7Qk](https://www.youtube.com/watch?v=9C_JWsyx7Qk) (Accessed 17.7.2025)

EHPA (European Heat Pump Association), 2025c. European heat pump market report. Available at: <https://www.ehpa.org/wp-content/uploads/2025/07/EHPA-Market-Report-2025-executive-summary.pdf> (Accessed 12.01.2026)

EU-2024/573. Regulation (EU) 2024/573 of the European Parliament and of the Council of 7 February 2024 on fluorinated greenhouse gases, amending Directive (EU) 2019/1937 and repealing Regulation (EU) No 517/2014. Available at: <https://eur-lex.europa.eu/eli/reg/2024/573/oj/eng> (Accessed 18.8.2025)

Eurostat, 2025. Natural gas price statistics. Available at: [https://ec.europa.eu/eurostat/statistics-explained/index.php?title=Natural\\_gas\\_price\\_statistics\\_-\\_Natural\\_gas\\_prices\\_for\\_non-household\\_consumers](https://ec.europa.eu/eurostat/statistics-explained/index.php?title=Natural_gas_price_statistics_-_Natural_gas_prices_for_non-household_consumers) (Accessed 18.7.2025)

Finnish Energy, 2025. Energy Year 2024 – District Heating. Available at: <https://energia.fi/en/statistics/statistics-on-district-heating/>. (Accessed 18.7.2025)

Herold, K.E., Radermacher, R. & Klein, S.A., 2016. Absorption Chillers and Heat Pumps. 2nd edition. Boca Raton: CRC Press.

HPTTCP, 2023. Annex 58 High-Temperature Heat Pumps Task 1 – Technologies Task Report. Heat Pump Centre.

IEA, 2025. World Energy Investment, 10th Edition. Available at: <https://iea.blob.core.windows.net/assets/d604d9db-9884-4449-a2df-8e7b5359ea91/WorldEnergyInvestment2025.pdf> (Accessed: 18.7.2025)

Jeßberger, J., Arpagaus, C., Heberle, F., Brendel, L., Betsch, S. & Brüggemann, D., 2024. Experimental investigations of upscaling effects of high-temperature heat pumps with R1233zd(E). International Journal of Refrigeration, 164, 234-256.

Jiang, J., Hu, B., Wang, R. Z., Deng, N., Cao, F., Wang, C-C., 2022. A review and perspective on industry high-temperature heat pumps. Renewable and Sustainable Energy Reviews 161, 112106.

Kaappola, E., Hirvelä, A., Jokela, M. & Kianta, J., 2023. Kylmätekniiikan perusteet. 5. painos. Opetushallitus. Punamusta Oy.

Klute, S., Budt, M., van Beek, M., Doetsch, C., 2024. Steam generating heat pumps – Overview, classification, economics and basic modeling principles. Energy Conversation and Management 299, 117882

Ma, X., Du, Y., Zhao, T., Zhu, T., Lei, B. & Wu, Y., 2024. A comprehensive review of compression high-temperature heat pump steam system: Status and trend. International Journal of Refrigeration, 164, 218-242.

Mansour, A. & Müller, N., 2019. A review of flash evaporation phenomena and resulting shock waves. Experimental Thermal and Fluid Science 107, 146-148.

Marina, A., Spoelstra, S., Zondag, H.A. & Wemmers, A.K. An estimation of the European industrial heat pump market potential. Renewable and Sustainable Energy Reviews, 139, 110545.

Ministry of Economic Affairs and Employment of Finland, n.d. Waste Heat. (Accessed 1.8.2025) Available at: <https://tem.fi/en/waste-heat>

Motiva Oy, 2019. Esiselvitys – Ylijäämälämmön potentiaali teollisuudessa. (Accessed 4.8.2025) Available at: [https://www.motiva.fi/files/16214/Esiselvitys\\_-\\_Ylijaamalammon\\_potentiaali\\_teollisuudessa.pdf](https://www.motiva.fi/files/16214/Esiselvitys_-_Ylijaamalammon_potentiaali_teollisuudessa.pdf)

- Rannikko, J. 2023. Kuumalämpöpumppujen hyödyntäminen teollisuuslämmöntuotannossa Suomessa. Bachelor's thesis, LUT University. Available at: <https://lutpub.lut.fi/handle/10024/165360>
- Rath, S. (2019) Syttyvät kylmäaineet. Vantaa: Suomen Kylmäyhdistys ry.
- Rontti, A. 2024. Kuumalämpöpumppujen prosessikytkentöjen vertailu. Master's thesis. LUT University. Available at: <https://lutpub.lut.fi/handle/10024/168573>
- Solla, T. 2025. Kuumalämpöpumppujen sekä kuumalämpöpumpun ja höyryn mekaanisen puristuksen COP-arvojen vertailu. Master's thesis. LUT University. Available at: <https://lutpub.lut.fi/handle/10024/169907>
- Sulaiman, A., Cotter, D., Arpagaus, C., & Hewitt, N. 2023. Theoretical Evaluation of Energy, Exergy, and Minimum Superheat in a High-Temperature Heat Pump with Low GWP Refrigerants. *International Journal of Refrigeration*, 153, 99-109.
- Sulaiman, A., Cotter, D., Xuan Le, K., Huang, M. & Hewitt, N. 2022. Thermodynamic analysis of subcritical High-Temperature heat pump using low GWP Refrigerants: A theoretical evaluation. *Energy Conversion and Management*, 268, 116034.
- Tolvanen, S. 2018. Estimating the effects of de-superheating spray on MVR fan performance using CFD. Master's thesis, LUT University. Available at: <https://lutpub.lut.fi/handle/10024/156484>
- Vahterus, 2020. Vahterus – 30 vuotta lämmönsiirtoa, Vahterus. Available at: <https://vahterus.com/fi/company/news/2020/vahterus-30-vuotta-1%C3%A4mm%C3%B6nsiirtoa> (Accessed 15.8.2025)
- Vahterus, n.d. How to transfer heat from liquid in a PSHE, Vahterus. Available at: <https://vahterus.com/applications/evaporators/> (Accessed 18.8.2025)
- Vavilov, A. 2025. Hiilivetyjen soveltuvuus teollisuuden kylmäaineiksi. Bachelor's thesis, Tampere University of Applied Sciences. Available at: [https://www.theseus.fi/bitstream/handle/10024/889388/Vavilov\\_Aleksanteri.pdf?sequence=2](https://www.theseus.fi/bitstream/handle/10024/889388/Vavilov_Aleksanteri.pdf?sequence=2)

Wang, P., Kowalski, S., Gao, Z., Sun, J., Yang, C.M., Grant, D., Boudreaux, P., Huff, S. & Nawaz, K. 2024. District heating utilizing waste heat of a data center: High temperature heat pumps. *Energy & Buildings*, 315, 114327.

Zini, A., Vaccaro, G., Rocchetti, A., Talluri, L. 2024. Working Fluid Selection for High-Temperature Heat Pumps: A Comprehensive Evaluation. *Energies* 2024, 17, 1556.